Int J Earth Sci (Geol Rundsch) (2010) 99:705–726
DOI 10.1007/s00531-009-0427-3

ORIGINAL PAPER

Neoproterozoic diamictite in the Eastern Desert of Egypt and Northern Saudi Arabia: evidence of ~750 Ma glaciation in the Arabian–Nubian Shield?

Kamal A. Ali · Robert J. Stern · William I. Manton · Peter R. Johnson · Sumit K. Mukherjee

Received: 27 February 2008 / Accepted: 5 February 2009 / Published online: 26 February 2009

Abstract The Neoproterozoic Atud diamictite in Wadi Kareim and Wadi Mobarak in the Eastern Desert of Egypt and the Nuwaybah formation in NW Saudi Arabia consist of poorly sorted, polymictic breccia, with clasts up to 1 m of granitoid, quartz porphyry, quartzite, basalt, greywacke, marble, arkose, and microconglomerate in fine-grained matrix. Stratigraphic relations indicate that the diamictite was deposited in a marine environment. Integrated field investigation, petrographic study and U–Pb SHRIMP zircon ages demonstrate that the Atud and Nuwaybah are correlative. The distribution of zircon ages indicate that ~750 Ma ages are dominant with a significant component of older materials, characterized by minor Mesoproterozoic and more abundant Paleoproterozoic and Neoarchean ages. Some matrix and metasedimentary clast zircons yield ages that are a few 10s of Ma younger than the age of the youngest clast (754 ± 15 Ma), suggesting Atud/Nuwaybah diamictite deposition ~750 Ma or slightly later, broadly consistent with being deposited during the Sturtian glaciation (740–660 Ma). The Paleoproterozoic and Neoarchean clasts have no source within the ensimatic Arabian–Nubian Shield. The distribution of the pre-Neoproterozoic ages are similar to the distribution of the pre-Neoproterozoic ages in Yemen and Saharan Metacraton, suggesting that these clasts have been transported hundreds of kilometers, maybe by ice-rafting. The Atud diamictite may represent important evidence for Cryogenian "Snowball Earth" in the Arabian–Nubian Shield.

Keywords Arabian–Nubian Shield · Snowball Earth hypothesis · Neoproterozoic · U–Pb SHRIMP zircon

Introduction

The Arabian–Nubian Shield (ANS) exposes Neoproterozoic (1,000–542 Ma) crust and extends from Egypt, Israel, and Jordan to Ethiopia and Yemen. The ANS (Fig. 1a) developed during fragmentation of Rodinia ~870 Ma and concluded ~620 Ma when convergence between East and West Gondwana closed the Mozambique Ocean along the East Africa–Antarctic Orogen (EAAO, Stern 1994; Jacobs and Thomas 2004). The northern part of the EAAO records the tectonic and magmatic evolution of the upper crust prior to, during, and after terminal collision (Stern 1994; Hargrove et al. 2006a, b).

The ANS is characterized by four main rock sequences: juvenile arc supracrustal sequences, ophiolites, gneissic core complexes, and granitoid intrusions (Abdel Naby et al. 2002; Shalaby et al. 2005). Such lithologies are well-exposed in the Eastern Desert of Egypt and in correlative exposures in NW Saudi Arabia. Because sedimentary rocks in ANS supracrustal sequences were deposited in a largely marine environment during important episodes of Neoproterozoic climate change (Fairchild and Kennedy 2007), these rocks should contain some evidence of these events. We are only beginning to examine ANS sedimentary successions for information about Neoproterozoic climate and

Electronic supplementary material The online version of this article (doi:10.1007/s00531-009-0427-3) contains supplementary material, which is available to authorized users.

K. A. Ali (✉) · R. J. Stern · W. I. Manton · S. K. Mukherjee
Department of Geosciences, University of Texas at Dallas, Richardson, TX 75080, USA
e-mail: kaa042000@utdallas.edu

P. R. Johnson
Geological Consulting, Johnson and Vranas Associates Ltd, 1242 Tenth Street, NW, Washington, DC 20001-4214, USA

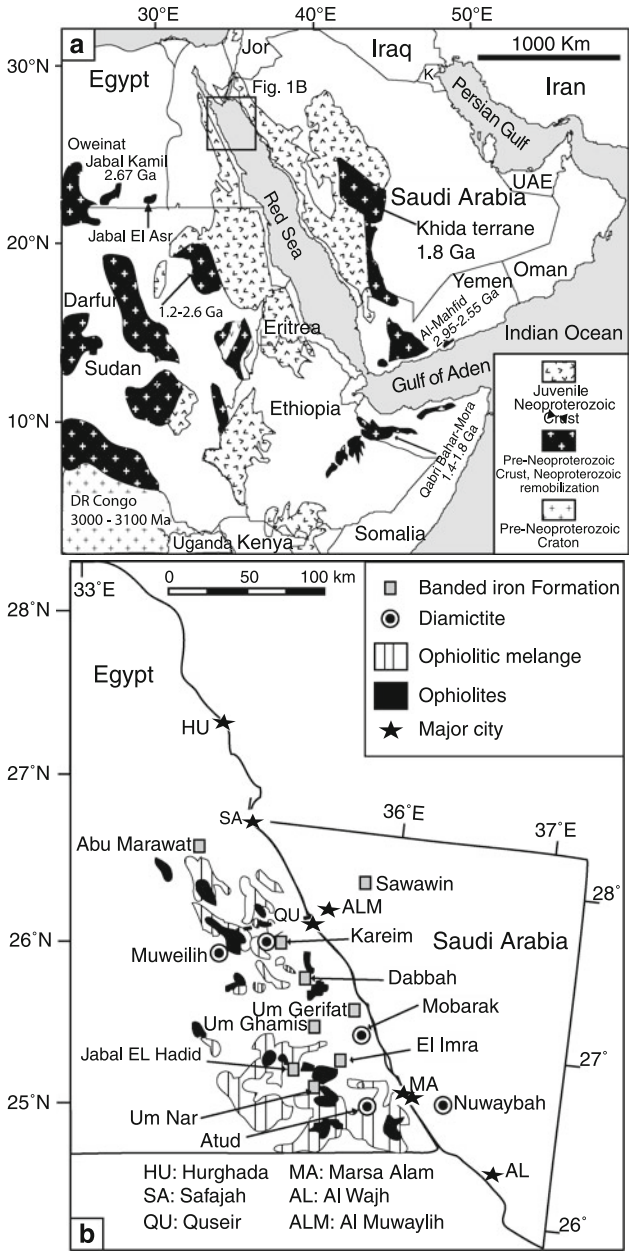

Fig. 1 **a** Map of the Arabian–Nubian Shield (Modified from Stern et al. 2006), showing the location of the study areas and regions where pre-Neoproterozoic crust is found. Ages for pre-Neoproterozoic crustal tracts are from Whitehouse et al. (1998); Sultan et al. (1994); Agar et al. (1992); Kröner and Sassi (1996); Stern et al. (1994) and Walraven and Rumvegeri (1993). **b** Location of the Neoproterozoic diamictite–BIF, and ophiolitic rocks in the northern Arabian–Nubian Shield, with the Red Sea closed (Modified after Sultan et al. 1993; Stern et al. 2006; Azer and Stern 2007)

related events (Stern et al. 2006). This report presents new data on a sequence of diamictite known as the "Atud diamictite" which may have formed during one of the Neoproterozoic glacial episodes.

One of the most interesting metasedimentary units in the northern ANS are the banded iron formations (BIF). Neoproterozoic BIF is one of the five "pillars" of the Snowball Earth hypothesis, articulated by Hoffman (2007) thus: "That the only regionally extensive sedimentary Fe_2O_3 and MnO_2 ores in the past 1.9 Ga are intimately associated with Cryogenian glacial marine deposits, implying exceptional perturbations in seawater chemistry, as expected if the oceans were ice covered for long periods". Neoproterozoic BIF is exposed in several areas in the Central Eastern Desert of Egypt (Sims and James 1984) and around Sawawin, Saudi Arabia (Goldring 1990; Fig. 1b). These are called "ANS-BIF" by Stern et al. (2006), who also noted that ANS-BIF and the Atud diamictite are components of a broadly Sturtian (~700 Ma) metasedimentary succession associated with Neoproterozoic ophiolites, and so were probably deposited in a relatively deep marine basin (Fig. 1b). It is thus important to better understand the depositional environment of the diamictite (i.e. glacial or non-glacial).

The Atud diamictite is also important because understanding the composition and age of clasts helps illuminate the nature of pre-Neoproterozoic crust in the region around and within the northern ANS. It is known that some relicts of pre-Neoproterozoic crust exist within the ANS. Intact Archean crust is known from exposures in Yemen (Whitehouse et al. 2001b) and Paleoproterozoic crust is preserved in the ~1.8 Ga Khida subterrane of the SE Arabian Shield (Fig. 1a) (Stacey and Agar 1985; Whitehouse et al. 2001a). Even in seemingly juvenile Neoproterozoic igneous rocks, ion–probe U–Pb dating of individual zircons reveals abundant xenocrystic zircons with ages of especially ~1.9 and ~2.5 Ga age (Hargrove et al. 2006a, b; Kennedy et al. 2004, 2005, 2007). Such zircons are common in metavolcanic rocks with Nd isotopic characteristics indicating derivation from melting of depleted (asthenospheric) mantle and geochemical characteristics suggesting formation in an intra-oceanic arc (Hargrove et al. 2006b). One possibility is that such ancient zircons are contributed by sediments to juvenile Neoproterozoic melts, so it is important to understand what ages of zircons are found in Neoproterozoic sediments.

Here we report the results of our studies of two occurrences of the Atud diamictite in the Central Eastern Desert of Egypt, at Wadi Kareim and Wadi Mobarak (Fig. 1b). We also document for the first time a correlative diamictite across the Red Sea in the Nuwaybah Formation of the Midyan terrane, NW Saudi Arabia (Nuwaybah diamictite). We report on the nature of the diamictite at these three localities including the results of petrographic and U–Pb zircon geochronologic investigations and use these results to interpret the origin of the Atud/Nuwaybah diamictite. We used the sensitive high mass-resolution ion microprobe with reverse geometry (SHRIMP-RG) specifically to determine U–Pb ages of individual zircons separated from

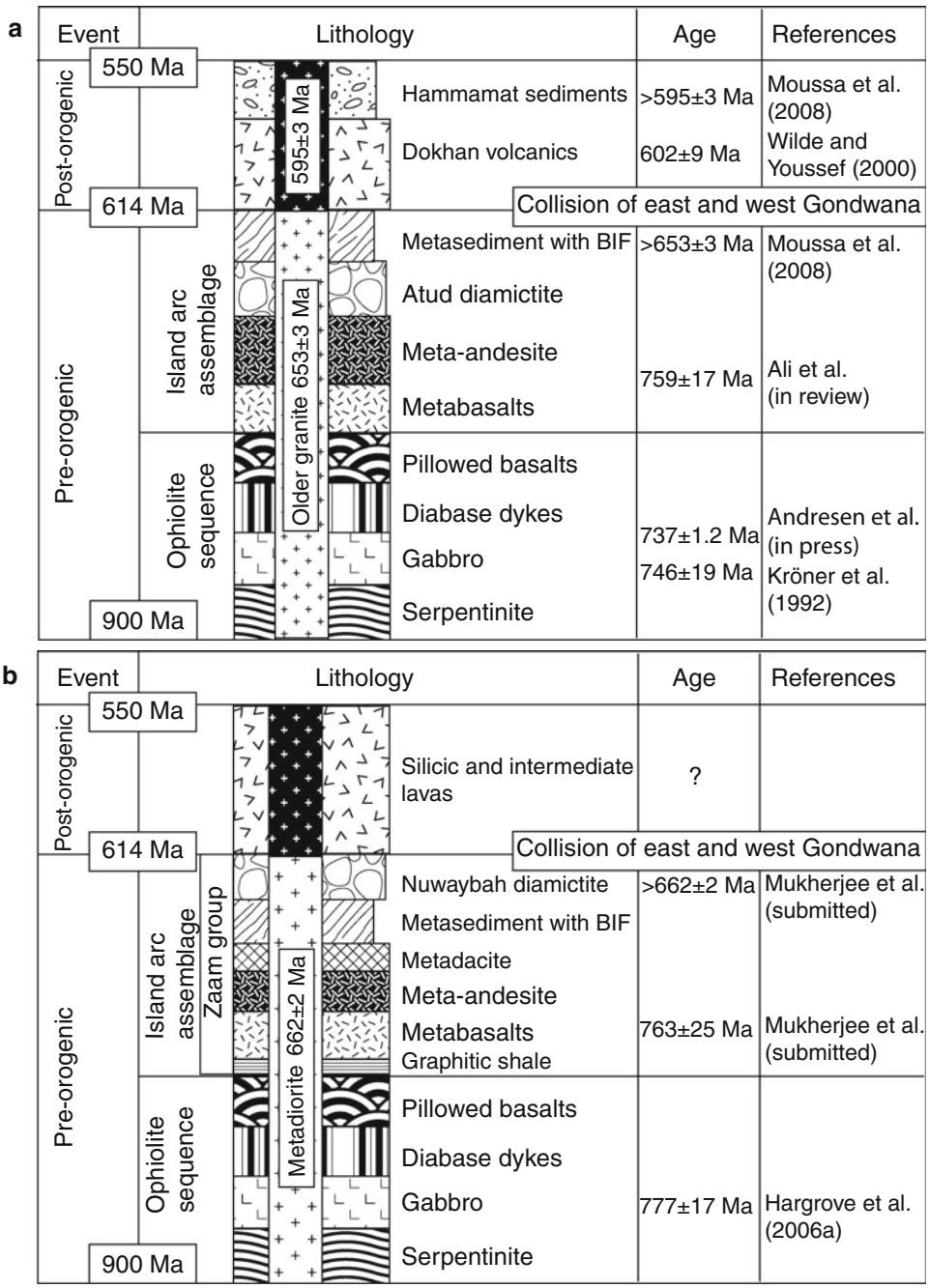

Fig. 2 **a** Lithostratigraphic and major tectonic events of the Neoproterozoic basement complex in Egypt (Modified from Stern 1981; Moghazi 2003). Ages from Kröner et al. (1992); Ali et al. 2008; Moussa et al. 2008; Wilde and Youssef 2000). **b** Lithostratigraphic and major tectonic events in NW Suadi Arabia. Ages from Hargrove et al. (2006); Mukherjee et al. (2009)

diamictite clasts and matrix. These ages are coupled with field observations to constrain the timing of diamictite units and to investigate their depositional environment.

Previous work

There are two conglomeratic units in the Neoproterozoic basement of Egypt, known as Atud Formation (El-Essawy 1964) and Hammamat Group (Fig. 2; Akaad and Noweir 1969). In spite of the fact that these units have very different occurrences, they are sometimes confused. The Atud Formation consists of massive poorly sorted and rounded clasts, from sand to boulder, in a sheared grey matrix (El-Essawy 1964); it was deposited ~700 Ma (Stern et al. 2006). Atud clasts include quartzite, highly altered granitoid, and a distinctive breccia; in contrast to the Hammamat Group, no clasts of ~600 Ma Dokhan volcanics or pink granite are observed (Akaad et al. 1996).

Abu El Ela (1990) studied the petrography and chemistry of Atud clasts east of Jabal Atud and suggested that these are compositionally similar to Dokhan volcanics and

calc-alkaline older granites. Abu El Ela (1990) concluded that Atud conglomerate is related to the Hammamat Group and not part of the older volcanic-arc assemblage because he could not explain how the clasts, which appear to have been derived from continental crust, could have been transported across a Neoproterozoic back arc basin. The conglomerate at Wadi Muweilih (Fig. 1b) was suggested to be related to the Atud Formation (Akaad and Noweir 1964; Akaad and Abu El Ela 1996) although it has also been considered as sheared Hammamat (Stern 1979; Ries et al. 1983). Akaad et al. (1996) studied the petrography and chemistry of Muweilih clasts and concluded that, because these lack clasts of Dokhan volcanics or pink granites, the Muweilih conglomerate is Atud, not Hammamat Group. They also concluded that the Muweilih conglomerate was deposited along a continental margin as a result of severe erosion of a volcano–plutonic orogen.

Stern et al. (2006) argued that the term "conglomerate" is not appropriate for the coarse-grained deposits of the Atud Formation. Texturally, the formation better fits the description of diamictite by Flint et al. (1960) as poorly sorted and very coarse terrigenous sediment. Eyles and Januszcak (2004) defined diamictite as poorly sorted deposits of boulders, gravel, silt and clay in a very fine-grained matrix, which is an apt description of the Atud Formation (Fig. 3). Diamictite forms in many sedimentary environments, for example as landslide deposits, in areas of submarine fans, on the slopes of volcanoes, and as meteorite ejecta blankets (Eyles and Januszcak 2004). In some cases, diamictite forms in glacial and glacially influenced environments. Convincing evidence of glacial origin would include striated clasts produced by glacial abrasion (Boulton 1978), dropstones released from melting icebergs (Ovenshine 1970) and far-traveled clasts (Eyles and

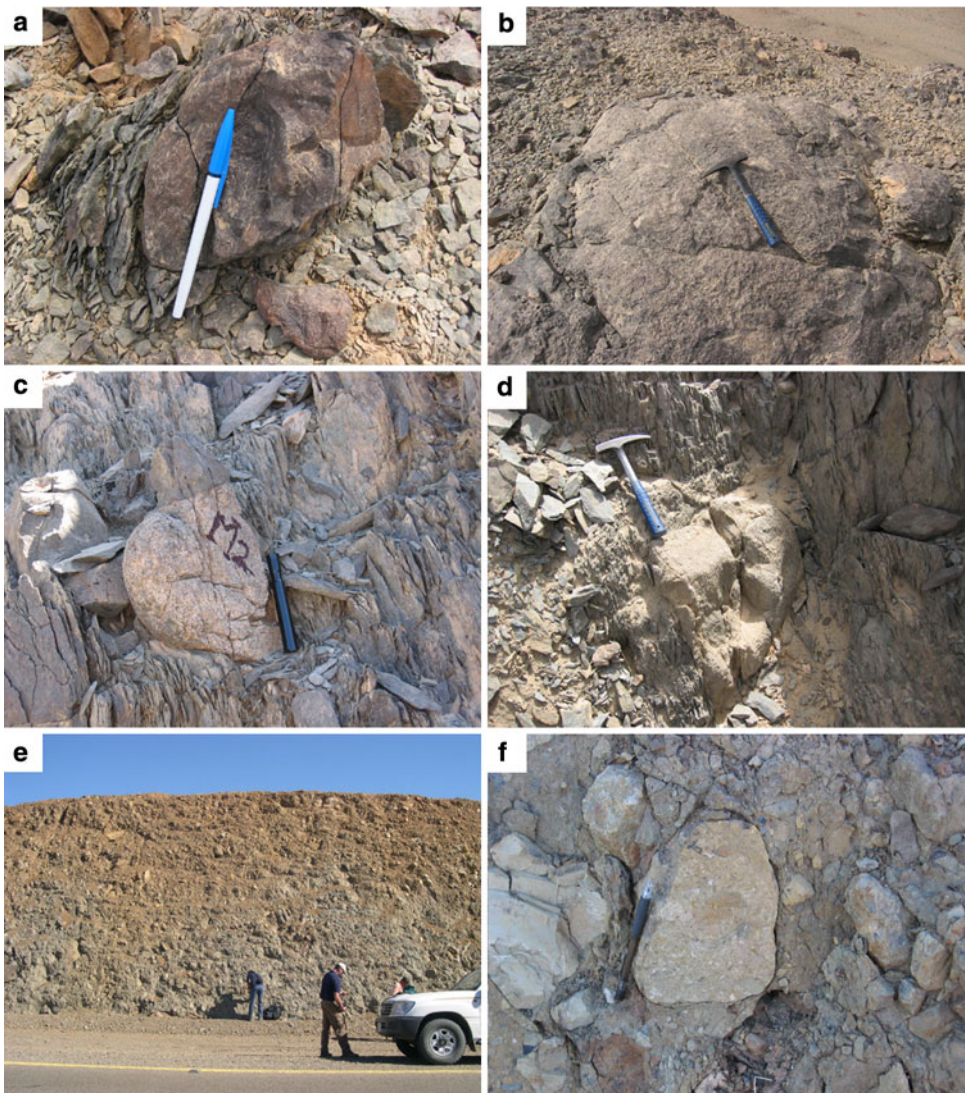

Fig. 3 Field photographs of Atud–Nuwaybah diamictite. **a** Atud diamictite arkose clast in fine-grained schistose matrix at Wadi Kareim, Egypt (*pen* for scale). **b** Atud diamictite microconglomerate clast in fine-grained schistose matrix at Wadi Kareim, Egypt (*hammer* for scale). **c** Atud diamictite granitoid clast in fine-grained schistose matrix at Wadi Mobarak, Egypt (*felt-tip marker* for scale). **d** Atud diamictite highly altered granitoid clast enclosed in metagreywacke laminations at Wadi Mobarak, Egypt (*hammer* for scale). **e** Nuwaybah diamictite outcrop along the Red Sea highway, NW Saudi Arabia. **f** Clast of microconglomerate in fine-grained matrix Nuwaybah formation, NW Saudi Arabia (*pen* for scale)

Januszcak 2004). We agree on this basis with Stern et al. (2006) that the unit is most appropriately referred to as the "Atud diamictite".

Confident determination of whether or not the Atud diamictite formed in association with glaciation requires evidence such as clast striations, faceted clasts, and/or dropstones, but such evidence is unlikely to be preserved because of the strong deformation that affected the Arabian–Nubian Shield. However, the Oman region, in the vicinity of the Arabian–Nubian Shield (Fig. 1a), was affected by Neoproterozoic glacial events. The Huqf Supergroup in northern Oman (Jabal Akhdar) and Mirbat Group in southern Oman record two important Neoproterozoic glaciations (Rieu et al. 2007). In Jabal Akhdar, the Abu Mahara Group, includes two glacial diamictite horizons (Le Guerroué et al. 2005), the Ghubrah Formation (712 ± 1.6 Ma, Leather 2001) and the overlying Fiq Formation (<645 Ma, Bowring et al. 2007). The marine siliciclastic Nafun Group overlying the Fiq Formation is constrained by U–Pb zircon ages from ashes and ignimbrite flows (c. 635–542 Ma, Allen and Leather 2006), so it appears that the Ghubrah Formation represents a Sturtian glaciation and the Fiq Formation represents a Marinoan glaciation (Le Guerroué et al. 2005; Allen and Leather 2006). The Ghubrah Formation diamictite is characterized by poor stratification; polymictic poorly sorted clasts and unsorted silty-shale matrix with some striated clasts (Le Guerroué et al. 2005). These general features are similar to the description of Atud diamictites.

Atud cobbles were previously concluded to have no source within the Eastern Desert of Egypt (Dixon 1981). Geochronologic data support the inference that Atud diamictite clasts sample much older rocks than are exposed in the Eastern Desert of Egypt and so must have been transported some distance. Two granitic cobbles from the NW of Marsa Alam (also referred to as the Wadi Mobarak metasedimentary unit) yielded highly discordant conventional U–Pb zircon upper intercept ages of 1,120 and 2,060 Ma (Dixon 1981). Dixon (1979) also obtained a discordant U–Pb zircon upper intercept of 2.3 Ga for a granitic cobble from Atud conglomerate outcrops in Wadi Kareim. From these results, Dixon (1981) inferred that the cobbles were transported from a region of pre-Neoproterozoic crust west of the present Nile River, possibly by ice-rafting.

Geological setting

There are four Atud diamictite occurrences known within the Central Eastern Desert of Egypt: Wadi Kareim, Wadi Mobarak, Wadi Muweilih, and the type locality east of Jabal Atud; we studied the first two occurrences. In addition, we document the first occurrence of correlative diamictite in once-adjacent parts of Saudi Arabia. As shown in Fig 1b, Atud diamictite, BIF, and ophiolite are spatially related, especially in Egypt, but BIF and diamictite only show a clear stratigraphic relationship at Wadi Kareim.

The Atud diamictite where we have studied it in Egypt and Saudi Arabia is poorly sorted, matrix-supported, polymictic and contains subrounded clasts up to a meter in size. It is distinctive in the field because its clasts are strikingly different from the ensimatic assemblages that characterize the Eastern Desert, and include grey quartzite, arkose, quartzite, felsic metavolcanics, granitoid, quartz porphyry, microconglomerate, basalt, and minor dark grey marble. The three areas of detailed study are discussed further below.

Atud diamictite (Wadi Kareim, Egypt)

The Wadi Kareim study area (Fig. 4a) is the only locality where the Atud diamictite was found in clear stratigraphic relationship with banded iron formation (Fig. 2a). The diamictite is part of a supracrustal succession with metavolcanics overlain by immature metasediments and BIF; the entire sequence is thrust over younger Hammamat conglomerate to the south. Younger metavolcanic rocks (classification of Stern 1981) at the base of the section are ~100 m thick and are truncated by the thrust; these metavolcanics are the subject of another study (Ali et al. 2008).Above the metavolcanic rocks, the Atud diamictite is succeeded by immature clastic sediments (wackestone and siltstone), which are succeeded upwards by the BIF.

Atud diamictite (Wadi Mobarak, Egypt)

The Wadi Mobarak study area (Fig. 4b) is characterized by east–west structures and lithologic belts distinct from the principal northwest–southeast trend of the Central Eastern Desert, which largely reflects the Najd Fault System (Shalaby et al. 2005). Basement exposures around Wadi Mobarak are dominated by highly deformed ophiolitic fragments of serpentinites, metagabbro, and greenschist-facies mafic metavolcanics while the metasedimentary sequence includes tuff, shale, schist and diamictite (Akaad et al. 1995), intruded by Neoproterozoic gabbro and granite. The diamictite appears to be repeated by thrusting. No BIF is found within the study area, which lies in the eastern part of Wadi Mobarak, but BIF is found at Um Nar farther west (Shalaby et al. 2005; Akaad et al. 1995).

Nuwaybah Formation (Saudi Arabia)

The Nuwaybah locality (Fig. 4c) is located within the Al Wajh quadrangle which lies between 26°00′ and 26°30′N

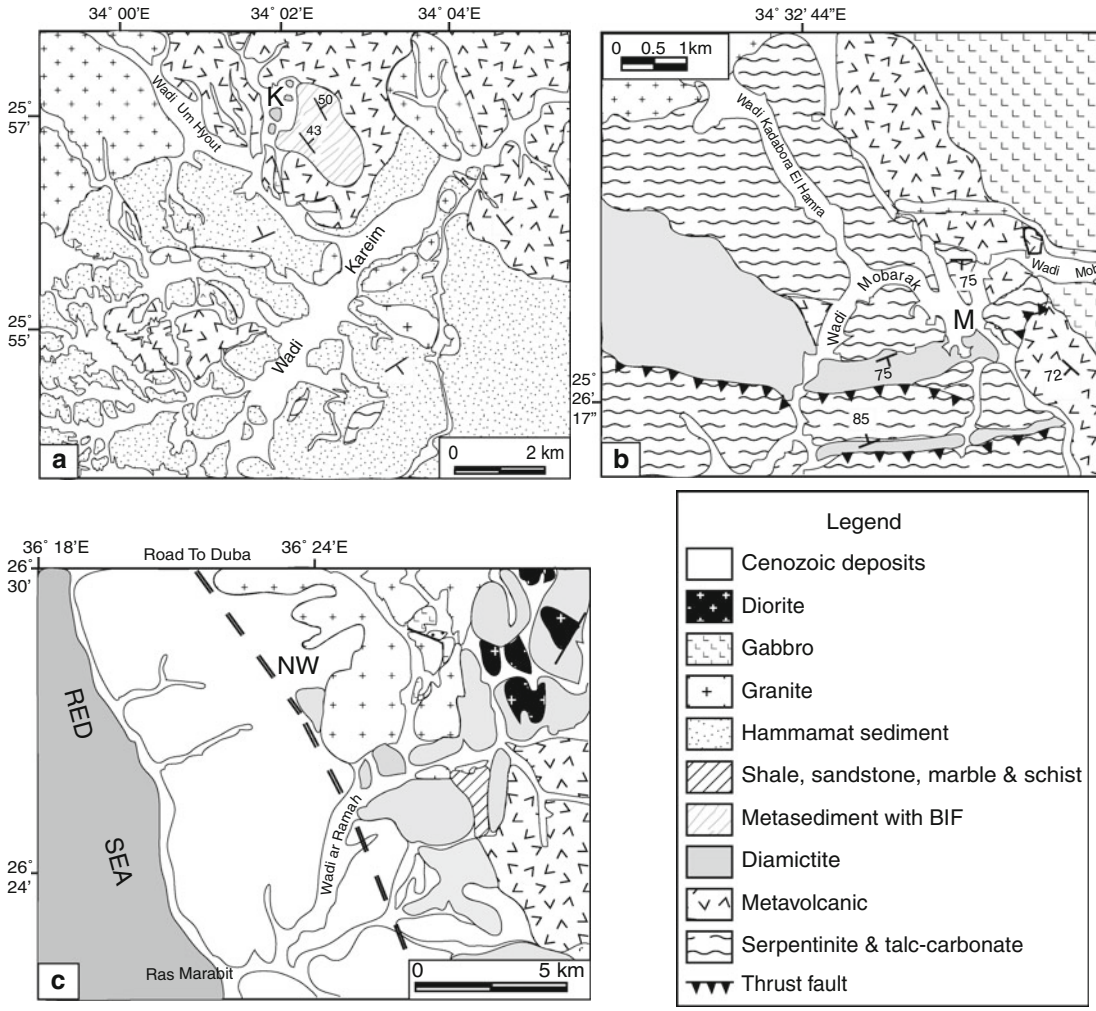

Fig. 4 Detailed geologic maps of Atud diamictite study areas. **a** Wadi Kareim, Central Eastern Desert of Egypt, showing the location of Atud diamictite and samples (K). **b** Wadi Mobarak, Central Eastern Desert of Egypt, showing the location of the diamictite samples (M). **c** Nuwaybah diamictite, Zaam group, NW Saudi Arabia, showing the location of diamictite samples and outcrop shown in Fig. 3c (NW)

and between 36°00′ and 37°00′E (Davies 1985). The diamictite is part of the Zaam Group (Fig. 2b), which consists of five units (shale, andesite, diamictite, sandstone and volcanic rocks). No BIF is found within the study area, but BIF is found at Wadi Sawawin farther north (Fig. 1b; Goldring 1990).

Research methods

Rock samples were collected during three field seasons in Egypt and Saudi Arabia in 2004, 2005, and 2006; sample locations are shown in Fig. 4. Thin section petrographic studies provided a basis for selecting samples for geochronologic studies (Table A1 in supplementary material). On this basis, we selected 17 samples (14 clasts and 3 matrix samples) for U–Pb zircon age determinations. This included nine samples from Wadi Kareim, Egypt, four samples from Wadi Mobarak, Egypt and four samples from Arabia.

Samples were processed at UTD to extract zircon using standard crushing and mineral separation techniques, including sieving size fractions, Wilfley table separation of heavy minerals, removal of magnetic fractions using a Frantz magnetic separator, and purification of zircons using heavy liquids.

Analytical work was performed during two sessions in 2005 and 2006 using the sensitive high mass-resolution ion microprobe with reverse geometry (SHRIMP-RG), co-managed by US Geological Survey and Stanford University Department of Geological and Environmental Sciences. A total of 229 spots on 229 zircons from 17 samples were determined. Analytical procedures are described in detail by Hargrove et al. (2006a, b). Analytical data acquired by SHRIMP-RG for all samples and apparent concordia ages are presented in Table A2 (supplementary

material). All samples are plotted as two-sigma error ellipses on Tera–Wasserburg concordia diagrams or on Wetherill concordia diagrams (Wetherill 1956; Tera and Wasserburg 1972; Figs. 6, 7, 8, 9). Representative cathodoluminescence images are shown in Fig. 10.

We report ages for clasts based on weighted mean ages for multiple zircon analyses from individual samples as well as ages for individual grains when no single age for the sample was obtained. Concordia ages are determined using ISOPLOT (Ludwig 2000). ISOPLOT determines two models based upon the calculated mean square of weighted deviates (MSWD) parameter. Model 1 uses assigned analytical errors and error correlations when these are the reasons for scatter; MSWD will be close to unity. Model 2 ages are reported when the MSWD is greater than unity, suggesting that there may be non-analytical error (Whitehouse et al. 1998). Ages for discordant zircons are reported as $^{238}U/^{206}Pb$ ages for ages <1.0 Ga and as $^{206}Pb/^{207}Pb$ ages for ages >1.0 Ga. To assess the most suitable filter for accepting or excluding ages, we plotted U–Pb zircon ages against U (ppm) and Th/U for all analysed zircons (as shown in Figure S1 in supplementary material). These plots show that there is no clear filter we can use, however the best filter we found is to exclude analyses which are discordant and/or show low Th/U (Th/U $\leq$ 0.3), high U (>500 ppm) and high common Pb. We treated each of the 17 samples separately because some show a clustering around certain age while other clast zircon populations show great scatter.

Diamictite lithofacies association and petrography

Diamictite lithofacies association

The Atud diamictite lithofacies may represent terrestrial moraine, tidewater, or marine glacial deposits. Detailed facies analysis is complicated by pervasive deformation. Nevertheless, the Atud Formation facies occurs within a succession of clastic sediments dominated by metaconglomerate and metagreywacke, with subordinate metamudstone. The lack of evidence for a basal unconformity and association with greywacke and BIF are most consistent with a marine or lacustrine depositional environment. Sedimentary lithofacies in moraine-mound complexes may have varied materials because the sheets of glaciers may flow over many rock units (Hambrey and Glasser 2002). Tidewater glaciers tend to rework glaciomarine facies, ranging from coarse gravel (ice-contact facies), to homogenous mud with dispersed clasts up to boulder size of ice-rafted origin (Hambrey and Glasser 2002). Confident interpretation of lithofacies is beyond the scope of this study, because deformation has obscured most primary sedimentary features. Nevertheless, interpretation of Atud diamictite lithofacies association is discussed below, adapted in part from (El-Essawy 1964; Allen et al. 2004). The Atud diamictite association at the type locality Jabal Atud occurs as an elongated outcrop about 6.7 km long and 2 and 3 km wide, whereas the Atud diamictite at Wadi Mobarak outcrops with a length of about 5 km and width of about 1 km. In Wadi Kareim the Atud diamictite association occurs as a few hills about 50 m wide and about 20 m high.

Conglomerate lithofacies

The metaconglomerate is clast-supported, beds are usually ~2–3 m thick, greenish grey in color and poorly sorted. The fine-grained conglomerate is dark grey, poorly sorted, and composed of rock fragments, quartz grains and feldspar embedded in microcrystalline groundmass. The rock fragments constitute >50% of the rock. Some conglomerate is composed of rock fragments less than 3 cm. The rock fragments are rounded to subrounded granules and pebbles and included volcanic, reworked metagreywackes, marble and cataclastic gneisses. Coarse-grained conglomerate contains clasts up to 2 m in diameter. Clasts are generally angular, ellipsoidal and flattened. Clasts include marble, granite, quartz porphyry, arkose and quartzite, and are described in detail below and in Table A1 (supplementary material).

Metagreywacke lithofacies

Metagreywacke occurs as massive, greenish grey layers 30 cm–2 m thick, with persistent mm-scale laminations. Clasts are angular and rounded ranging from 10 to 75 cm, composed of different lithologies, and are enclosed by metagreywacke laminations. Clasts include marble, granite, quartz porphyry, greywacke, arkose and quartzite. The metagreywacke laminations are defined by variations in the proportion of rock fragments and quartz in a fine-grained matrix of quartz and calcite.

Metamudstone lithofacies

Metamudstones occur as a subordinate facies up to 25 cm thick, with persistent mm-scale pencil-like splinters (El-Essawy 1964). The metamudstones are interbedded with the metaconglomerates and metagreywackes. In the type locality (Jabal Atud), the metamudstones do not occur throughout the entire facies associations but are abundant in the middle part of the unit (El-Essawy 1964).

Size and petrography of diamictite clasts

Atud diamictite clasts are weakly embedded in a scaly greywacke matrix. Figure 5 presents scans of thin sections

and photomicrographs for representative clast lithologies described in this section.

(a) *Granitoid* Clasts are rounded to subrounded and are brownish, grey or reddish. Granitoid clasts are composed of subhedral to anhedral, highly strained quartz (Fig. 5a). The feldspars are anhedral and highly altered, so that plagioclase and K- feldspar cannot be distinguished. Biotite and hornblende are replaced by chlorite, and calcite occurs as patches within feldspar.

(b) *Quartz porphyry* These are fine-grained, grey, and composed of corroded euhedral quartz grains, with chert and volcanic fragments embedded in a fine-grained matrix (Fig. 5b). The volcanic fragments are composed of quartz and altered plagioclase; albite twining could be recognized.

(c) *Basalt* These are dark grey, fine-grained clasts composed of altered plagioclase, clinopyroxene, and groundmass of the same minerals (Fig. 5c). The plagioclase occurs as subhedral phenocrysts, recognized by albite

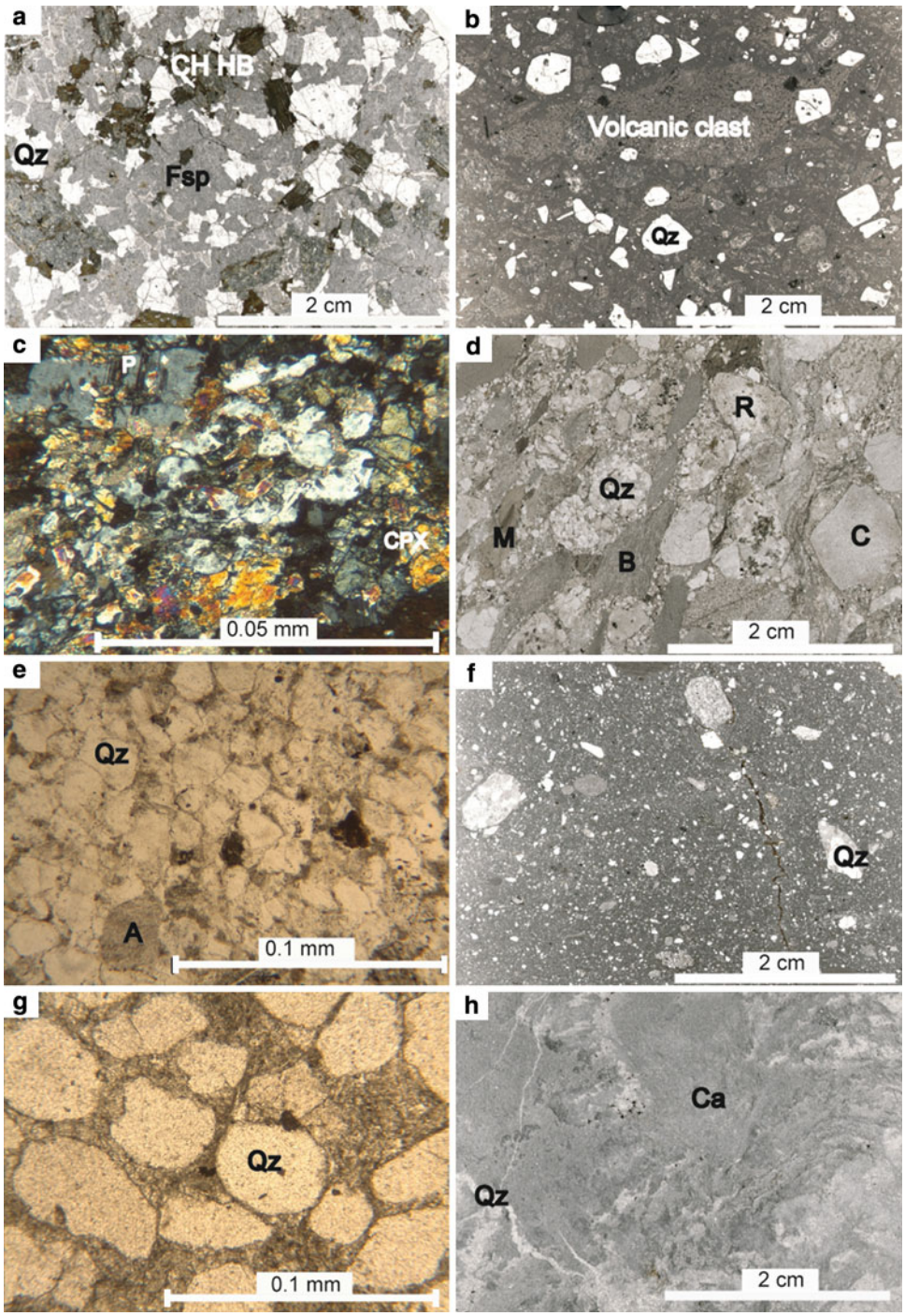

Fig. 5 Photomicrographs and scans of diamictite clasts. **a** Granitoid K2B scan. **b** Quartz porphyry M9 scan. **c** Basalt M11 photomicrograph. **d** Microconglomerate K1A scan. **e** Arkose NCB photomicrograph. **f** Greywacke K1D scan. **g** Quartzite K2D photomicrograph. **h** Marble M15 scan. *Qz* quartz, *CH* chlorite, *HB* hornblende, *Fsp* feldspar, *R* rhyolite, *B* basalt, *C* chert, *Ca* calcite, *M* mudstone, *CPX* clinopyroxene, *A* alkali feldspar, *P* plagioclase

twining. The clinopyroxene occurs as phenocrysts, showing strong interference colors.

(d) *Microconglomerate* This distinctive clast type consists mostly of gravel-sized rock fragments, with ~75% pebbles of rhyolite, basalt, trachyte, chert and mudstone in an arkosic matrix of quartz, feldspar, mica and chlorite (Fig. 5d). The cementing material is mostly calcite, with subordinate quartz.

(e) *Arkose* This is a fine-grained clastic sediment. Quartz occurs as angular to subrounded grains, feldspars are subordinate and chlorite is found as scattered grains (Fig. 5e). The most common accessory minerals are zircon, rutile and magnetite. The cement is made of interlocking carbonate and quartz.

(f) *Greywacke* This clast type is light to dark grey in color, fine-grained and composed mainly of angular to subrounded grains of quartz and fragments of chert and granitoid fragments in a fine-grained matrix (Fig. 5f). The matrix consists of mica, chlorite and unidentified detrital material.

(g) *Quartzite* These are hard, fine-grained, grey rocks, in which abundant quartz grains are cemented by carbonate (Fig. 5 g). Grains are 95 % or more rounded quartz, marked by small inclusions of impurities.

(h) *Marble* This fine-grained rock is massive and grey, mainly composed of anhedral calcite with many thin calcite and quartz veinlets. Scattered quartz grains form a mosaic with calcite (Fig. 5 h).

Geochronological results

Table 1 summarizes the geochronological results. Table 2 compares the most important geochronologic results for the three localities. Results from each of these sites are discussed further in the following sections.

Wadi Kareim (Egypt)

The nine samples from Wadi Kareim include eight clasts from the diamictite (5 granitoid clasts, 1 quartzite, 1quartz porphyry, and 1 arkose) and a matrix sample. The five granitoid clasts yield a range of ages, including two clasts with only Neoproterozoic (~750 Ma) zircons; one clast that yielded mostly Neoproterozoic (750–790 Ma) zircons along with abundant 2.1–2.4 Ga zircons; a clast that yielded a Paleoproterozoic age (2006 ± 15 Ma), which appears to have been reset in Neoproterozoic time and a clast that yielded only Paleoproterozoic–Archean ages. The quartz porphyry yielded mostly Neoproterozoic ages (697–778 Ma) along with one early Paleoproterozoic and one Archean zircon. The quartzite clast yielded Paleoproterozoic to Archean (2,093–2,732 Ma) zircons. The arkose contained Neoproterozoic (~722–773 Ma) and older Paleoproterozoic zircons (1.8–2.5 Ga). The diamictite matrix contains zircons that were derived from a mixed Neoproterozoic and Paleoproterozoic sources. Further details on a sample-by-sample basis are given in the following paragraphs.

K2B is a subrounded, coarse-grained granitoid clast. One analysis of each of twenty-one zircons was performed, and the results are shown on a Tera–Wasserburg concordia diagram (Fig. 6a). These zircons have moderate U contents and low common ^{206}Pb. The analyses are mostly concordant and yield only Neoproterozoic ages ranging from 688 to 783 Ma. Data for all 21 zircons does not yield a good age but removing discordant data points and those with Th/U <0.3 yields a robust Model 2 (Ludwig 2000) lower intercept age based on 12 grains of 754 ± 15 Ma (2σ, MSWD = 2). K2B is one of the few clasts that do not contain any pre-Neoproterozoic zircons, providing the best older age limit for the depositional age of the diamictite. Still, five of fifteen concordant zircons give younger ages: 678 ± 6, 688 ± 7, 729 ± 7, 730 ± 6, 732 ± 6, suggesting that the clast may be significantly younger than 754 ± 15 Ma.

K2C is a subrounded and coarse-grained granitoid clast. One analysis was conducted for each of eight zircons, yielding ages that range from 545 to 2,441 Ma (Fig. 6b) with no concentration that allows a single age to be calculated. The three discordant zircons have significant (3–8%) common ^{206}Pb. A similar scatter of ages is observed if only the five concordant ages are considered, although a cluster of ages ~758–788 Ma based on three grains probably approximates the age of the granitoid. We note that the very young zircon (545 ± 3 Ma) has high U contents (556 ppm) and do not think it constrains the age of the diamictite. We infer that this clast was eroded from a granitoid which crystallized about 750–790 Ma and the four older ages (2.1–2.4 Ga) to represent Paleoproterozoic xenocrystic zircons picked up by the granitic magma.

K2E is a coarse-grained granitoid clast. One analysis was conducted on each of ten zircons, with ages ranging from 700 to 767 Ma, one of which was omitted because it was discordant. The remaining nine points plot on concordia in positions that suggest minor loss of radiogenic Pb. The nine points yield a Model 1 (Ludwig 2000) lower intercept age of 763 ± 45 Ma (2σ, MSWD = 1.6; Fig. 6c), which we interpret to indicate the crystallization age of the granitoid from which the clast was eroded. One zircon gave a significantly younger age (700 ± 9 Ma). This clast is like K2B, both petrographically and in terms of its age, lacking evidence of pre-Neoproterozoic zircons.

K2H is a granitoid clast. One analysis was conducted for each of ten zircons, which range in age from 1,654 to 1,986 Ma; all but one age (~1,986 Ma) are discordant

Table 1 Geochronological summary for Atud–Nuwaybah diamictite samples

Location	Sample No.	Latitude longitude	Lithology	Concordia ages	Concordant ages (Ma)
Wadi Kareim "Egypt"	K2B	25°56′59″ 34°02′00″	Granitoid	754 ± 15 (L.I)	
	K2C	25°56′59″ 34°02′00″	Granitoid	No concordia	545 ± 5
					758 ± 13
					769 ± 8
					788 ± 8
					2,432 ± 8
	K2E	25°56′59″ 34°02′00″	Granitoid	763 ± 45 (L.I)	
	K2H	25°56′59″ 34°02′00″	Granitoid	634 ± 57 (L.I) 2,006 ± 15 (U.I)	
	K2J	25°56′59″ 34°02′00″	Granitoid	No concordia	1,970 ± 19
					2,018 ± 48
					2,534 ± 24
					2,537 ± 27
					2,865 ± 23
					2,899 ± 79
					2,943 ± 27
	K1E	25°56′58″ 34°01′56″	Quartz porphyry	752 ± 33	
	K2D	25°56′59″ 34°02′00″	Quartzite	No concordia	2,093 ± 22
					2,107 ± 18
					2,597 ± 27
					2,732 ± 18
	K2G	25°56′59″ 34°02′00″	Arkose	No concordia	722 ± 5
					748 ± 7
					753 ± 9
					773 ± 5
					1,811 ± 20
					2,489 ± 11
					2,523 ± 13
	K1F	25°56′58″ 34°01′56″	Greywacke Matrix	No concordia	661 ± 8
					719 ± 9
					729 ± 8
					739 ± 9
					854 ± 10
					984 ± 12
					987 ± 12
					2,057 ± 12
					2,115 ± 12
					2,457 ± 14
					2,462 ± 19
					2,466 ± 9
					2,471 ± 12
					2,490 ± 26
					2,668 ± 20
Moubarak Egypt	M1	25°25′47″ 34°33′56″	Granitoid	770 ± 12 (L.I)	

Table 1 continued

Location	Sample No.	Latitude longitude	Lithology	Concordia ages	Concordant ages (Ma)
	M2	25°25′47″	Granitoid	831 ± 21 (U.I)	
		34°33′56″			
	M16	25°25′47″	Quartzite	1,224 ± 7	1,213 ± 11
		34°33′56″			1,220 ± 9
					1,222 ± 14
					1,226 ± 12
					1,227 ± 13
					1,243 ± 12
					2,418 ± 17
					2,468 ± 17
					2,505 ± 11
					2,514 ± 15
	M17	25°25′47″	Greywacke	No concordia	538 ± 6
		34°33′56″	Matrix		634 ± 8
					682 ± 9
					728 ± 9
					772 ± 10
					782 ± 13
					819 ± 9
					1,090 ± 13
					2,529 ± 13
					2,747 ± 14
Nuwaybah NW Arabia	NCA	26°27′00″	Granitoid	765 ± 22 (U.I)	
		36°24′00″			
	NCC	26°27′00″	Granitoid	No concordia	741 ± 16
		36°24′00″			742 ± 9
					1,753 ± 13
					2,084 ± 20
					2,704 ± 30
					2,747 ± 27
					2,883 ± 14
	NCB	26°27′00″	Arkose	766 ± 5 (Mean)	
		36°24′00″			
	NM	26°27′00″	Greywacke	No concordia	713 ± 17
		36°24′00″	Matrix		740 ± 10
					752 ± 13
					757 ± 15
					768 ± 25
					903 ± 18
					1,017 ± 20
					1,706 ± 16
					2,429 ± 61
					2,482 ± 13

(Fig. 6d). Many of these zircons have high U contents (>300 ppm) and high common ^{206}Pb, consistent with the observation of strong discordance. Nine zircons define a discordia (MSWD = 1.6) with an upper intercept of 2,006 ± 15 Ma and a poorly defined Neoproterozoic lower intercept of 634 ± 57 Ma. We are not sure if the ~2.0 Ga age reflects the intrusion/cooling age of Paleoproterozoic granite body reset during Neoproterozoic time or whether

Table 2 Summary of geochronological results for diamictite samples from Wadi Kareim, Wadi Mobarak, Egypt and Nuwaybah Formation, NW Saudi Arabia

Clasts	Wadi Kareim, Egypt	Wadi Mobarak, Egypt	Nuwaybah formation, Saudi Arabia
Granitoid	li = 754 Ma	li = 770 Ma	ui = 765 Ma
	li = 763 Ma	ui = 831 Ma	~741 Ma to ~2.8 Ga
	li = 634 (Ma)–ui = 2.0 Ga		
	~1.9–3.0 Ga		
	~7.58–2.4 Ga		
Quartz porphyry	li = 752 Ma–ui = 1.9 Ga		
Arkose	~722 Ma to ~2.5 Ga		766 Ma (Mean age)
Quartzite	~2.1 to ~2.7 Ga	~ 1.2 to ~2.5 Ga	
Matrix (greywacke)	~719 Ma to ~2.67 Ga	~ 634 Ma to ~2.7 Ga	~713 Ma to ~2.7 Ga

ui upper intercept, *li* lower intercept

the Neoproterozoic lower intercept approximates or intrusion/cooling age of a Neoproterozoic granitoid from which the clast was eroded that massively assimilated ~2.0 Ga crust, but tentatively prefer the first interpretation.

K2J is a granitoid clast. One analysis was conducted for each of nine zircons, which range in age between 1970 and 3155 Ma (Fig. 6e). All except the 1,970 Ma zircon contain very little U (7–55 ppm) and Th (0.04–3 ppm), and have very low Th/U, which suggests these may have experienced significant metamorphism. Seven analyses are concordant, ranging in age from 1,970 to 2,900 Ma; with a four grain cluster of ages between 2.8 and 2.95 Ga. The data do not yield a robust crystallization or metamorphic age, but it is most likely that this clast was eroded from a pre-Mesoproterozoic intrusion that could have been as old as 3.0 Ga and been metamorphosed as many as three times; certainly there is an imprint of ~1.9 Ga metamorphic or igneous activity but no hint of a Neoproterozoic overprint.

K1E is fine-grained quartz porphyry clast. One analysis was conducted on each of ten zircon grains, which range from 697 to 2,728 Ma; two of the ten grains yielded Paleoproterozoic or Archean ages. All zircons show moderate U contents, high Th/U indicating igneous origin, and only two zircons have significant common ^{206}Pb (697 ± 28, 724 ± 6 Ma). A Model 2 solution (Ludwig 2000) yielded a lower intercept age of 752 ± 33 Ma and upper intercept age of 1,957 ± 150 Ma (2σ, MSWD = 2.9; Fig. 6f) after excluding the three discordant zircons. We interpret this age to represent eruption or hypabbyssal emplacement of Neoproterozoic felsic magma that was contaminated by Paleoproterozoic and Archean materials.

K2D is a quartzite clast. One analysis was conducted for each of seven zircons, which range in age from 2.1 to 2.7 Ga. Four grains are concordant (Fig. 7a) and range from 2,098 ± 15 to 2,733 ± 19 Ma; the three discordant grains have significant common ^{206}Pb. Because it contains no Neoproterozoic zircons, we infer that this quartzite clast was eroded from a sedimentary quartzite bed that was deposited before Neoproterozoic time and that was derived from detritus shed by an ~2.1 Ga or older crustal tract.

K2G is a fine-grained arkose clast. One analysis was conducted for each of ten grains and yielded 8 concordant ages that range from 722 to 2,523 Ma (Fig. 7b); four concordant zircons range from 722 to 773 Ma, one is ~1.8 Ga and a three grain cluster is ~2.5 Ga. We are not sure of the significance of the 722 ± 5 Ma age; this is ~30 Ma younger than the age of the youngest clast (K2B). This clast was eroded from a lithified bed of coarse arkosic detritus derived from a mixed provenance of Neoproterozoic (~722–773 Ma) and older (Paleoproterozoic and Archean; 1.8–2.5 Ga rocks. This arkosic deposit thus was deposited, lithified, and then re-eroded and re-deposited some time after ~750 Ma, perhaps after ~720 Ma.

K1F is a sample of the greenish greywacke diamictite matrix. One analysis was conducted for each of 23 zircon grains, producing ages that range from 661 to 2,668 Ma (Fig. 7c). Discordant grains generally have the highest common ^{206}Pb. Sixteen of the analyses are concordant and range in ages from 719 to 854 Ma (5 grains), 984 to 987 Ma (2 grains), 2,059 to 2,115 Ma (2 grains), 2,458 to 2,503 Ma (6 grains), and 2,668 Ma (1 grain). We are not sure of the significance of the young (661 ± 8 Ma) age; this has significant common ^{206}Pb and moderate Th/U (0.22). The matrix sample does not yield an easily interpreted concordia age but indicates derivation from a mixed source of Neoproterozoic, Paleoproterozoic and Neoarchean sources.

Wadi Mobarak (Egypt)

We processed four samples from the diamictite at Wadi Mobarak: three clasts and the matrix. Two granitoid clasts yielded Neoproterozoic ages (770 ± 12, 831 ± 21 Ma); whereas one quartzite clast gave pre-Neoproterozoic ages (1.2–2.5 Ga). The matrix contains zircons that were derived from a mixture of Neoproterozoic, Paleoproterozoic and Neoarchean sources, similar to the results for the diamictite matrix at Wadi Kareim. Further details of these analyses are given below.

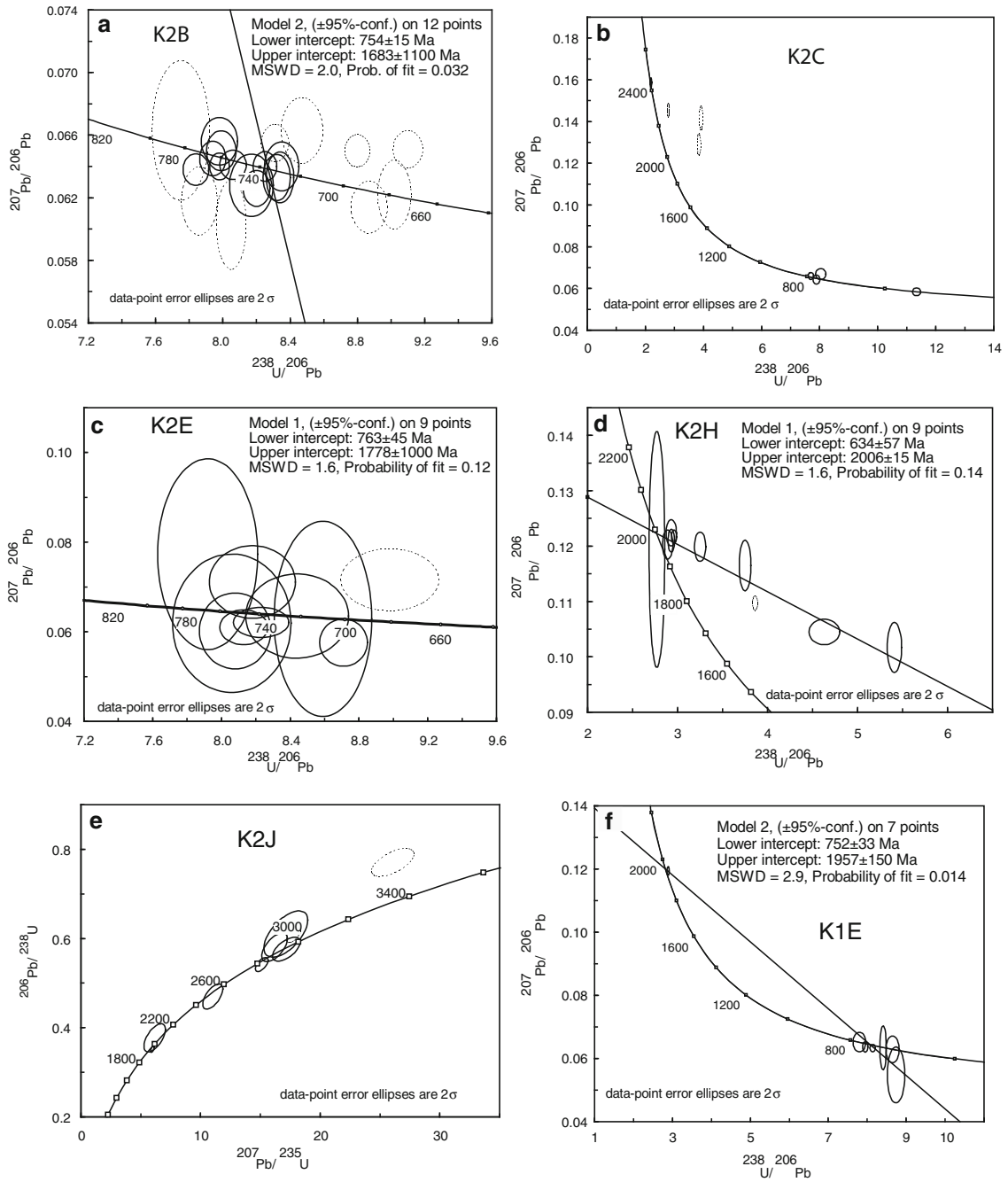

Fig. 6 U–Pb concordia diagrams for SHRIMP–RG data from Wadi Kareim igneous clasts. **a** K2B granitoid. **b** K2C granitoid. **c** K2E granitoid. **d** K2H granitoid. **e** K2J granitoid. **f** K1E quartz porphyry. Error ellipses are 2σ; weighted average age errors quoted at 95% confidence. *Dashed ellipses* indicate zircon analyses that were excluded from age calculations. Sample information is given in Table A1 and analytical data in Table A2 (supplementary material)

M1 is a coarse-grained granitoid clast. One analysis was conducted for each of 15 zircon grains and the analyses are plotted on Tera–Wasserburg concordia diagram (Fig. 8a). A few samples have high common ^{206}Pb, including a concordant age of 697 ± 32 Ma. Concordant zircons yield only Neoproterozoic ages that range from 697 to 805 Ma, although two discordant grains suggest an upper intercept age of ~2.7 Ga. Data for four zircon grains are excluded because three are discordant and one has large error due to high ^{204}Pb, The remaining 11 points define a Model 2 (Ludwig 2000) lower intercept age of 770 ± 12 Ma (±95% confidence, MSWD = 2.4; Fig. 8a). Weighted average ages for 11 concordant analyses yield a mean ^{207}Pb/^{206}Pb age of 777 ± 7 Ma (±95% confidence, MSWD = 1.33). We

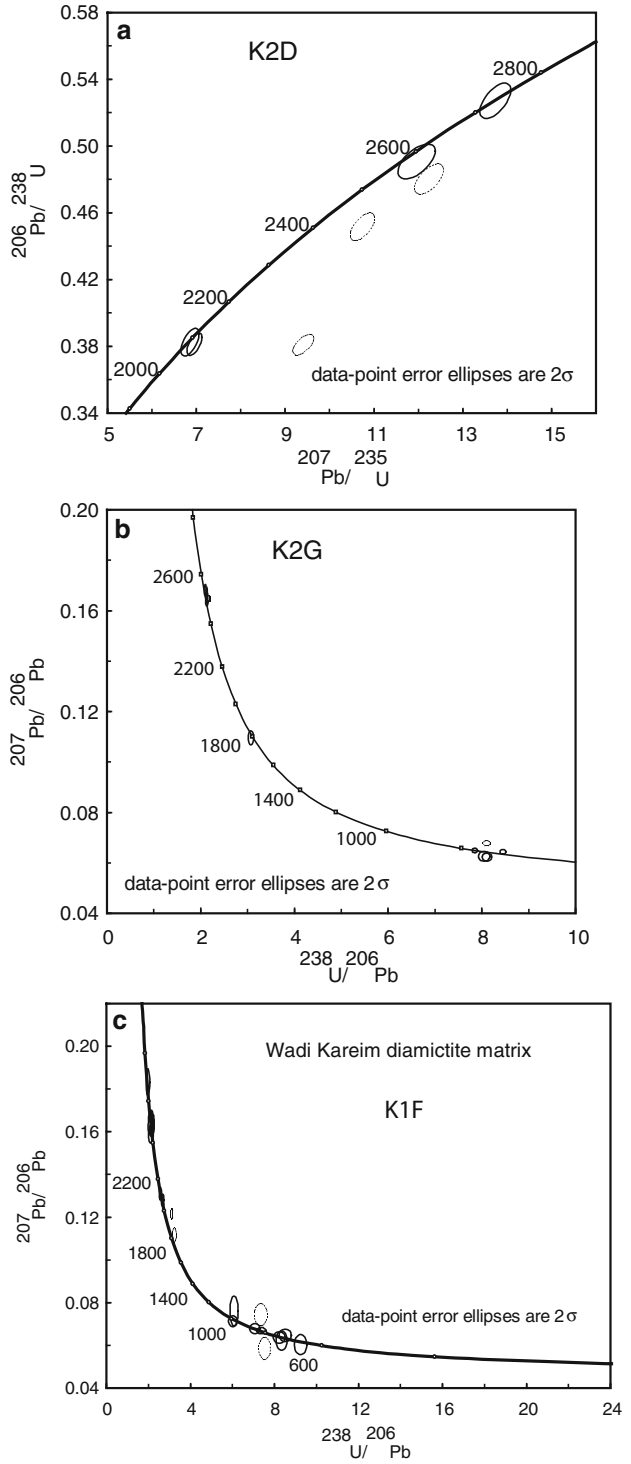

Fig. 7 U–Pb concordia diagrams for SHRIMP–RG data from Wadi Kareim diamictite samples. **a** K2D quartzite clast. **b** K2G arkose clast. **c** K1F diamictite matrix. Error ellipses are 2σ; weighted average age errors quoted at 95% confidence. Sample information is given in Table A1 and analytical data in Table A2 (supplementary material)

interpret this to represent the crystallization age for the granitic body from which this clast was derived. This clast age also indicates that the diamictite at Wadi Mobarak was deposited after ~770 Ma. This is slightly older than but consistent with the maximum age of 754 ± 15 Ma inferred for the deposition of the diamictite at Wadi Kareim, based on the age of granitoid clast K2B.

M2 is a coarse-grained granitoid clast. One analysis was conducted for each of 14 zircon grains, which range in age from 678 to 1,149 Ma; all but 3 ages are discordant (Fig. 8b), probably due to radiation damage caused by high U contents (mostly >1,000 ppm) of these zircons and reflected in mostly high common ^{206}Pb. The 1,149 Ma age is not considered to have geologic significance because it is reversely discordant and has high common ^{206}Pb. Three grains are concordant but are young (640–686 Ma), possibly erroneously due to very low Th/U (640 ± 8 Ma) and high common ^{206}Pb (666 ± 8, 686 ± 8 Ma). A discordia is defined with a Model 1 (Ludwig 2000) lower intercept age of 136 ± 42 Ma, which we consider to be geologically meaningless, and an upper intercept of 822 ± 32 Ma (2σ, MSWD = 1), which we interpret to approximate the crystallization age of the granitoid from which the clast was eroded.

M16 is quartzite clast. One analysis was conducted for each of 20 zircon grains, which range in age from 1,209 to 3,515 Ma (Fig. 8c). These mostly have high Th/U, show a large range in U contents, and mostly have low ^{206}Pb. There are no Neoproterozoic zircons. Eleven analyses are concordant and range in age from 1,213 to 2,514 Ma. One cluster of six grains yields a concordia age of 1,224 ± 7 Ma (±95% confidence, MSWD = 0.33). These zircons define a Model 2 (Ludwig 2000) lower intercept age of 1,239 ± 64 and upper intercept age of 2,456 ± 100 Ma (±95% confidence, MSWD = 40). This sample was eroded from a quartzite that itself was derived from a crustal tract composed of Mesoproterozoic, Paleoproterozoic and Neoarchean rocks. This quartzite is similar to the Kareim quartzite clast in lacking Neoproterozoic ages but has a different population of pre-Neoproterozoic ages, especially in having abundant Mesoproterozoic zircons, and is distinct from quartzite K2D in this regard.

M17 is the diamictite matrix. One analysis was conducted for each of 20 zircons, ranging in age from 539 to 2,752 Ma (Fig. 8d). Thirteen analyses are concordant, and these mostly range in age from 538 ± 6 to 819 ± 9 Ma (7 points), 1,090 ± 13 Ma (1 point), 2,504 ± 9 to 2585 ± 15 Ma (3 points) and 2,747 ± 14 Ma (1 point). Three concordant zircons give young ages: one is 538 ± 6 Ma, but has a very low Th/U, suggesting that it is metamorphic and for this reason is excluded from further consideration; the 682 ± 9 Ma age may be erroneous due to high common ^{206}Pb; the 634 ± 8 Ma age is also young but no obvious problem with this analysis can be seen. Like the diamictite matrix at Wadi Kareim, this sample does not yield a simple concordia age but indicates derivation from

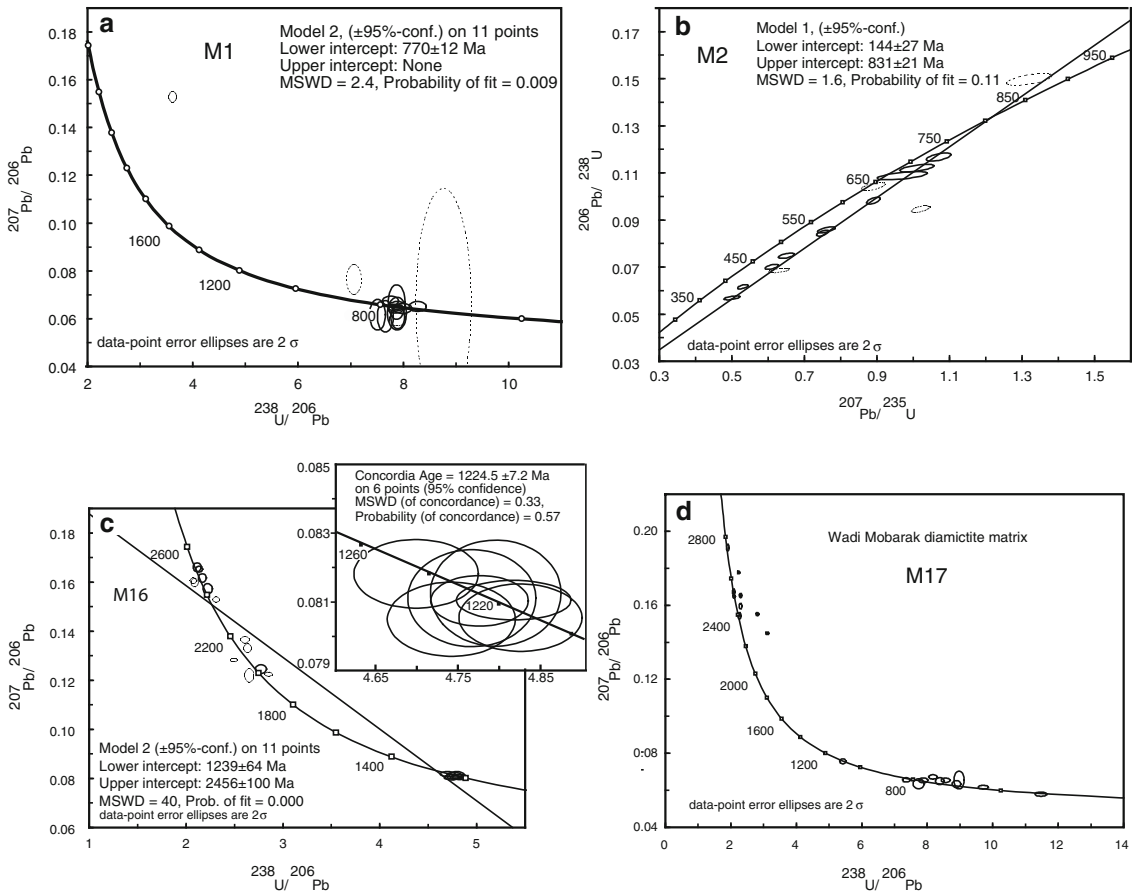

Fig. 8 U–Pb concordia diagrams for SHRIMP–RG data from Wadi Mobarak diamictite samples. **a** M1 granitoid clast. **b** M1 granitoid clast. **c** M16 quartzite clast. **d** M17 diamictite matrix. Error ellipses are 2σ; weighted average age errors quoted at 95% confidence. Sample information is given in Table A1 and analytical data in Table A2 (supplementary material)

a mixed source of mostly Neoproterozoic, Mesoproterozoic, and Neoarchean sources. Except for the absence of Paleoproterozoic zircons, these results are similar to those for the Kareim diamictite matrix.

Nuwaybah formation (Saudi Arabia)

We processed four samples from the Nuwaybah diamictite in Saudi Arabia: two granitoid clasts, an arkosic clast, and a matrix sample. One of the granitoid clasts and the arkosic clast yielded Neoproterozoic ages of 765 ± 22 and 766 ± 5 Ma respectively. A third granitoid clast was from a Neoproterozoic (~742 Ma) pluton that contained a lot of older (Paleoproterozoic and Archean) zircons. The Nuwaybah diamictite matrix contains zircons that were derived from a mixed source of Neoproterozoic, Paleoproterozoic, and Neoarchean sources, with a few ~1 Ga zircons.

NCA is a coarse-grained granitoid clast. One analysis was conducted for each of 12 grains, which showed low common ^{206}Pb and moderate U contents. All zircons yielded Neoproterozoic ages, from 767 to 816 Ma (Fig. 9a). Three analyses are excluded because of low Th/U (≤0.3); the other nine grains regressed together yield a Model 1 (Ludwig 2000) upper intercept age of 765 ± 22 Ma (2σ, MSWD = 1.3), which we interpret to reflect the age of the pluton from which this clast was derived. This is analytically indistinguishable from the maximum age of 754 ± 15, 763 ± 45 and 770 ± 12 Ma for similar Neoproterozoic granitoid cobbles from Wadi Kareim (K2B, K2E) and Wadi Mobarak (M1), respectively, all of which lack pre-Neoproterozoic zircons.

NCC is a coarse-grained granitoid clast. One analysis was conducted for each of 12 zircon grains, which range in age from 742 to 2,951 Ma. Seven analyses are concordant (Fig. 9b) and range widely in age: 741 ± 16, 742 ± 9, 1,753 ± 25 , 2,084 ± 39, 2,704 ± 30, 2,747 ± 27, and 2,883 ± 14 Ma. We interpret this age distribution to indicate that this clast was eroded from a Neoproterozoic (~741 Ma) granitic pluton that also contained a lot of Paleoproterozoic and Archean zircons.

NCB is a fine-grained arkose clast. One analysis was conducted for each of 12 zircon grains, which ranged in age from 620 to 2,074 Ma. Ten analyses are concordant ranging from 707 to 886 Ma (Fig. 9c). Seven data points

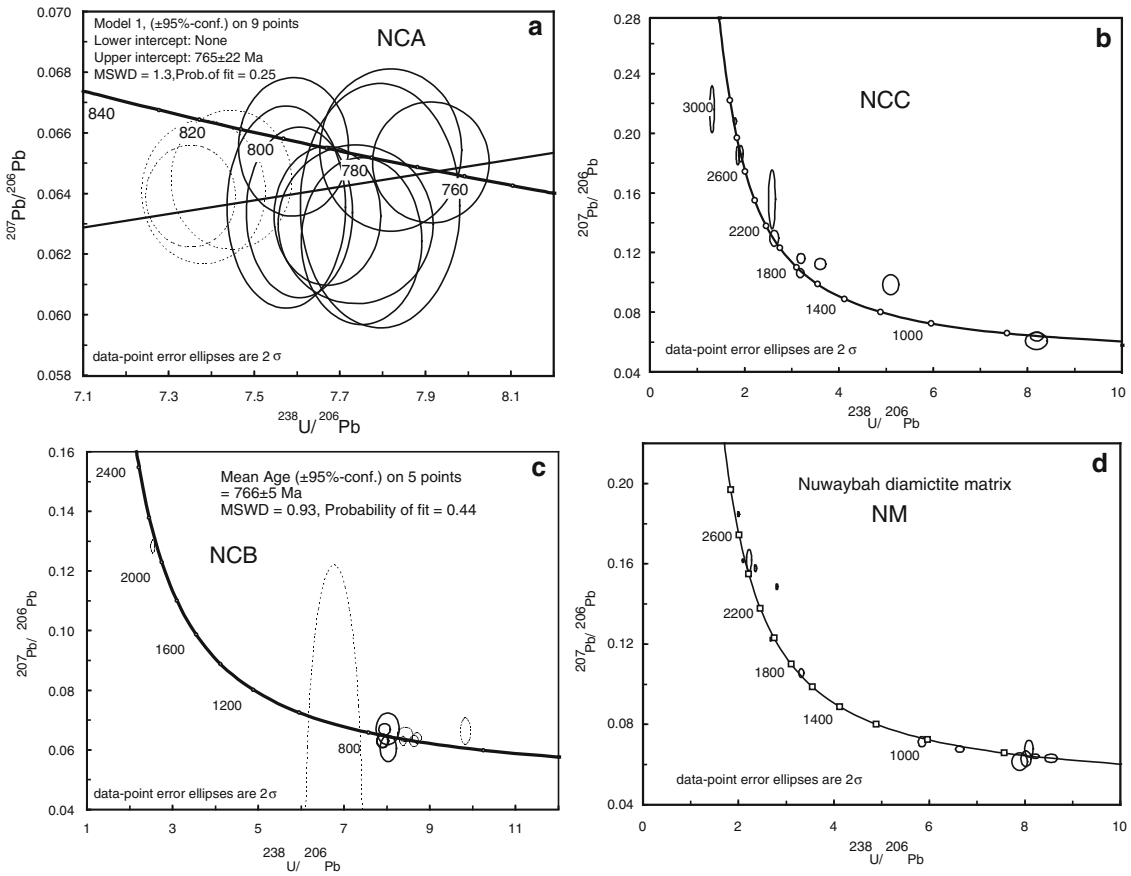

Fig. 9 U–Pb concordia diagrams for SHRIMP–RG data from Nuwaybah diamictite samples. **a** NCA granitoid clast. **b** NCC granitoid clast. **c** NCB arkose clast. **d** NM diamictite matrix. Error ellipses are 2σ; weighted average age errors quoted at 95% confidence. Sample information is given in Table A1 and analytical data in Table A2 (supplementary material)

are excluded because of discordance or high U content, but a five-grain cluster yields a mean age of 766 ± 5 Ma (95% confidence, MSWD = 0.93), which we interpret as the age of detritus shed from a mixed provenance dominated by Neoproterozoic and subordinate older (Paleoproterozoic) rocks. This arkose is similar to arkose K2G of Wadi Kareim in the Eastern Desert of Egypt.

NM is a sample of the fine-grained matrix diamictite matrix. One analysis was made for each of 14 zircon grains, which range in age from 713 to 2,696 Ma (Fig. 9d). Ten analyses are concordant and range in age from 713 to 2,482 Ma, but there is only one good cluster of ages, 740–768 Ma based on four grains. This distribution of ages indicates derivation from a mixed source of Neoproterozoic and Paleoproterozoic, sources, with a smattering of ~1.0 Ga ages.

Discussion

Below we briefly discuss several significant points resulting from our study: (1) observations of zircon morphology and appearance; (2) correlation of the Atud diamictite across the Red Sea; (3) age constraints for deposition of the Atud diamictite; and (4) origin significance of pre-Neoproterozoic clasts in the Atud diamictite.

Zircon morphology and appearance

The morphology of Atud diamictite zircons and their appearance in cathodoluminescence images (Fig. 10) reveals striking differences between Neoproterozoic zircons and Paleoproterozoic and Archean igneous and detrital zircons. Neoproterozoic igneous zircons (Fig. 10a, b, c) are euhedral, elongated, and show well-developed growth zoning. In contrast, older igneous zircons (Fig. 10g, h, i) sometimes have xenocrystic cores mantled by overgrowths or occur as unmantled subrounded or rarely euhedral crystals (Corfu et al. 2003). Detrital zircons (Fig. 10d, e, f) in quartzite appear very dark, perhaps due to high U contents. These commonly contain inclusions and rounded cores with zoning. Detrital zircon grains sometimes are fractured.

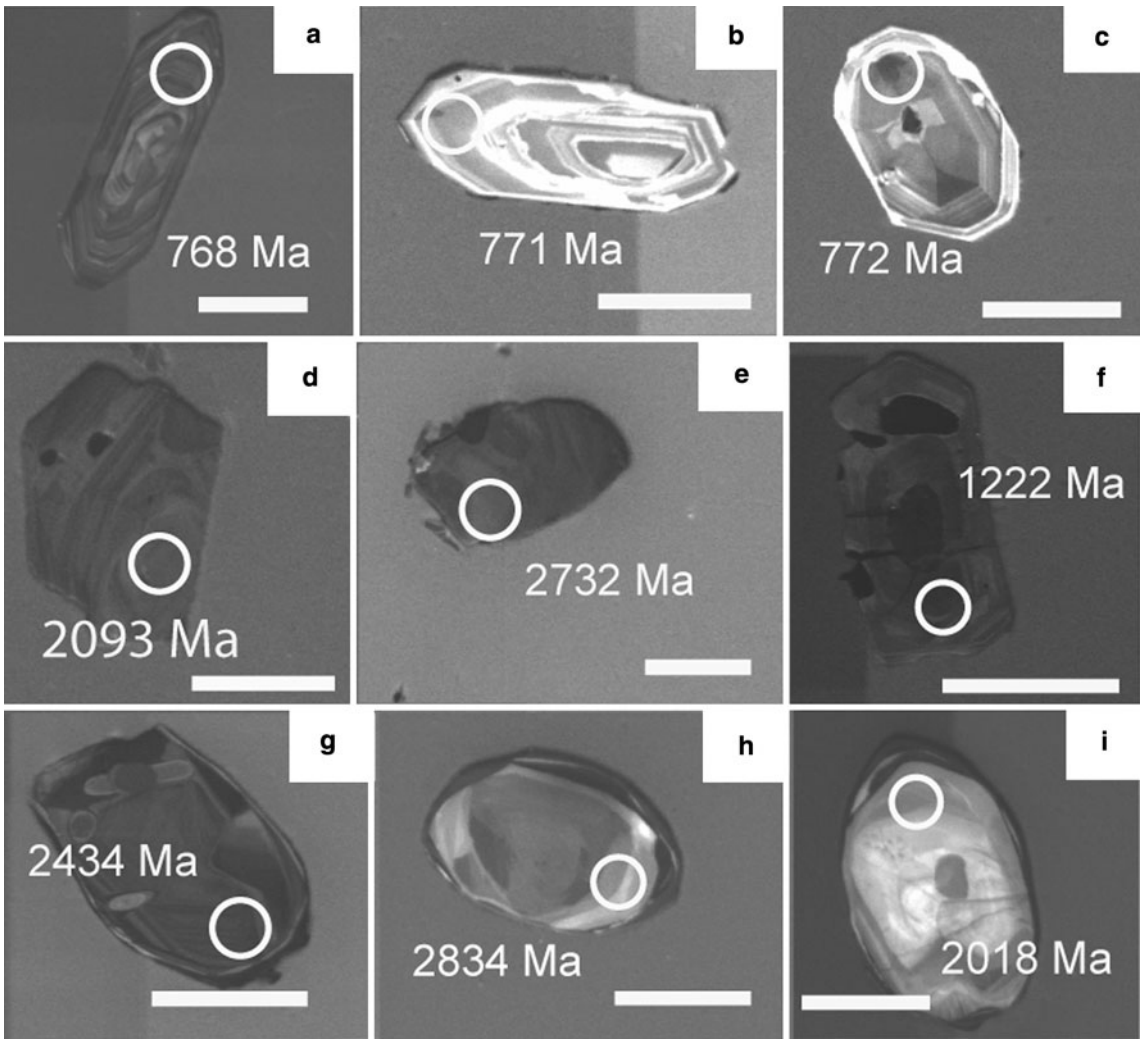

Fig. 10 Cathodoluminescence images of zircons from Atud diamictite clasts. **a, b** and **c** Typical Neoproterozoic igneous zircon grains from granitoid clast M1. **d, e** and **f** Typical quartzite zircon grains from clasts K2D and M16. **g, h** and **d** Typical zircon grains of igneous Paleoproterozoic and Archean from granitoid clasts K2C and K2J. Location of ion microprobe area is shown by *white circles; white scale bar* is 100 μm long

Correlation of the Atud diamictite across the Red Sea

There has been very little correlation of Neoproterozoic basement units across the Red Sea, beyond a general correlation of ophiolites and banded iron formation. This is partly due to the lack of distinctive lithologies in the Neoproterozoic basement of Egypt and NW Saudi Arabia and partly due to insufficient high-quality geochronologic information. Results of the present study provide a new opportunity to advance the trans-Red Sea correlation effort.

It has been noted that the diamictite exposed in Egypt is similar in field appearance and clast lithologies to the Nuwaybah diamictite exposed in Saudi Arabia. Field and petrographic study of the clasts within the diamictite suggests that the lithologies and size of the clasts at Wadi Kareim and Wadi Mobarak (Atud diamictite) in Egypt and Nuwaybah Formation in NW Saudi Arabia are similar. The distribution of zircon ages for the diamictite in Wadi Kareim and Wadi Mobarak, Egypt (Fig. 11a, b) is also very similar to those of the Nuwaybah diamictite in Saudi Arabia (Fig. 11c). These histograms show that ~690–825 Ma material dominated at all three locations, with a significant component of older materials (~2 and ~2.5 Ga). Table 2 further summarizes the similarity in ages of the granitoids for the three locations. Figure 12d is a compilation of all zircon ages from this study and emphasizes the point that all zircon grains analysed during this study are dominated by ~750 Ma ages with subordinate but still important Paleoproterozoic and Archean sources. Zircon ages for matrix at the three locations show similar distributions to each other and to the clasts and range from 713 Ma to 2.7 Ga (Fig. 11e), although the

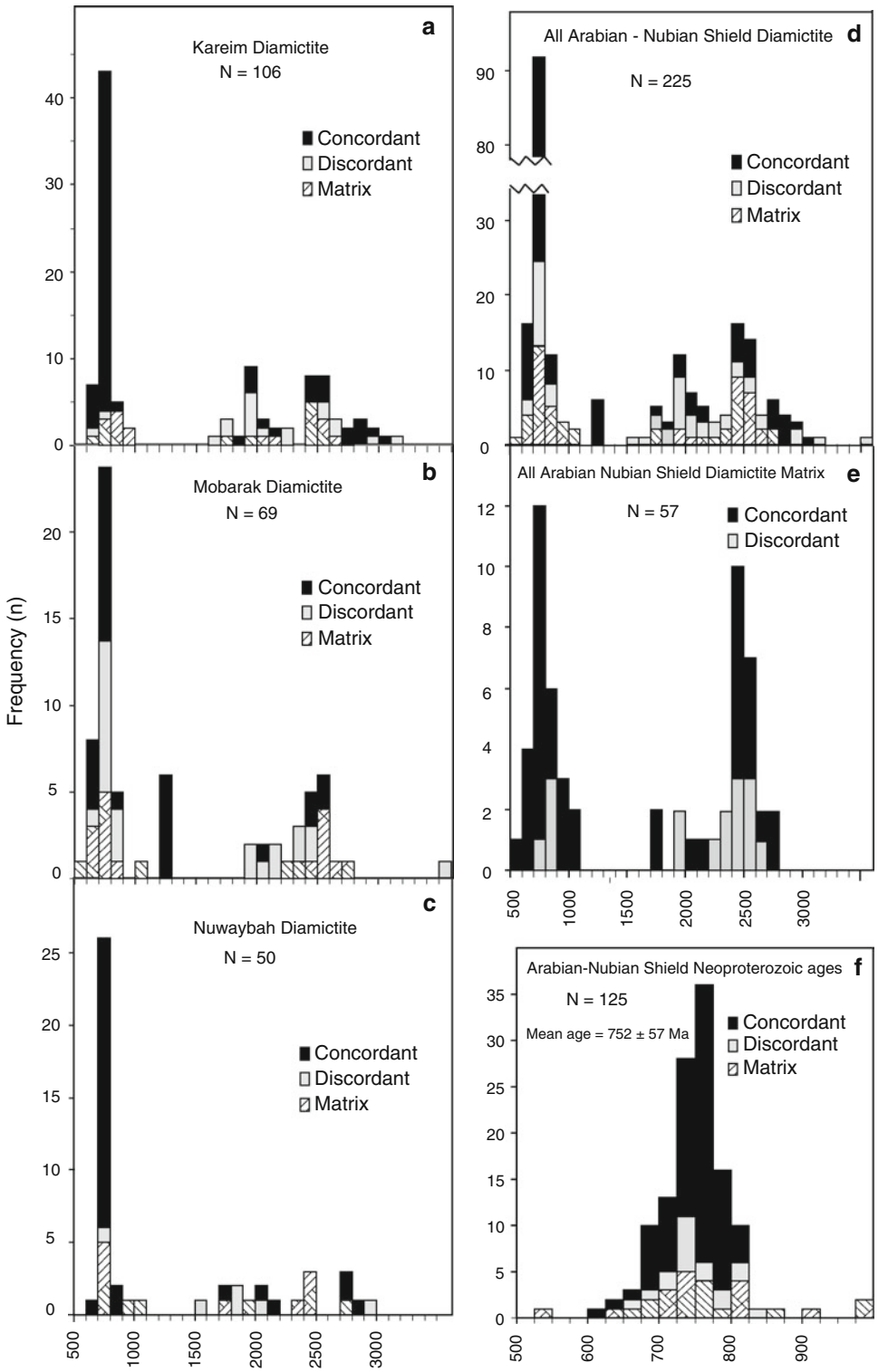

Fig. 11 Histograms of single-grain SHRIMP-RG zircon ages analysed during this study. **a** Wadi Kareim, Egypt. **b** Wadi Mobarak, Egypt. **c** Nuwaybah, Arabia. **d** Distribution of all zircon ages from this study, note secondary peaks at ~ 1.9 and ~ 2.5 Ma. Concordant and discordant applies to zircons separated from clasts in **a**–**d**. **e** Summary of age distributions for diamictite matrix zircons from all three localities. **f** Summarizes distribution of Neoproterozoic ages only, separated into concordant clast, discordant clast, and matrix. Discordant ages <1,000 Ma are $^{238}U/^{206}Pb$ ages and those >1,000 Ma are $^{207}Pb/^{206}Pb$

relative proportion of older zircons seems to be greater for the matrix than the clasts. The most obvious difference between the three sites is the presence of 1.1–1.2 Ga zircons in the Wadi Mobarak zircons, the only strong evidence that Mesoproterozoic rocks might have existed in the diamictite source region. The diamictite was clearly derived from a region or regions that had abundant ~750 Ma igneous activity (Fig. 11f). We conclude that the diamictite units that we have studied at the three localities are correlative and provide an important new stratigraphic marker within the otherwise monotonous metasedimentary section of the region and across the Red Sea.

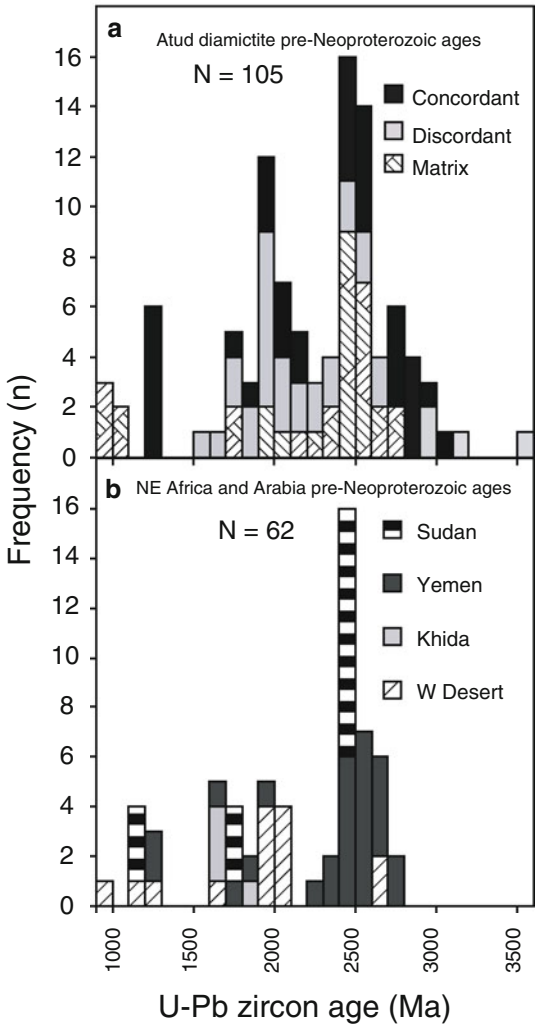

Fig. 12 Comparative histograms of single-grain zircon ages analysed during this study and ages for pre-Neoproterozoic outcrops around the Arabian–Nubian Shield. **a** Histogram showing the distribution of Atud diamictite pre-Neoproterozoic ages from this study. **b** Histogram showing distribution of pre-Neoproterozoic ages obtained for rocks from surrounding regions in western Egypt, northern Sudan, and southern Saudi Arabia, from Whitehouse et al. (1998); Sultan et al. (1994); Agar et al. (1992) and Stern et al. (1994). Discordant ages <1,000 Ma are $^{238}U/^{206}Pb$ ages and those >1,000 Ma are $^{207}Pb/^{206}Pb$ ages. Note the similar distributions observed for these histograms; the implications of this are further explored in the text

Age constraints for deposition of the Atud diamictite

It is not possible to directly determine the depositional age of diamictite, but this can be confidently constrained as being younger than the youngest clast. One clast within the Nuwaybah diamictite was eroded from a granitoid that crystallized at 765 ± 22 Ma. A Nuwaybah arkose clast yields an age 766 ± 5 Ma, which must be the age of the source granite from which the arkose was recycled. Kareim granitoid clasts yield crystallization ages of 754 ± 15 and 763 ± 45 Ma (lower intercept), whereas a quartz porphyry clast is 752 ± 33 Ma (lower intercept). A granitoid clast from Wadi Mobarak yields an age of 770 ± 12 Ma. The results for all the three localities thus indicate that the diamictite was deposited after ~760 Ma ago.

These age constraints are consistent with U–Pb zircon ages for the underlying metavolcanics. Ali et al. (2008) report an age of 759 ± 17 Ma for the metavolcanics at Wadi Kareim, which lie beneath the diamictite. In the field, the contact appears to be conformable but strong deformation may mask a significant hiatus, allowing the diamictite deposition to be significantly younger than the metavolcanics.

Individual grains in metasedimentary clasts and diamictite matrix may provide additional information. These grains passed the filter we suggested, some of these individual grains show younger ages than the age we concluded from the youngest clast (752 Ma). These ages range from 634 ± 8 to 740 ± 10 Ma which may indicate that the diamictite deposition age is younger than the age of the youngest clast suite (~760 Ma).

The maximum age constraints presented above are broadly consistent with deposition during the Sturtian glacial interval, which consisted of several glacial episodes during a protracted interval, 740–660 Ma ago (Fairchild and Kennedy 2007). There are younger episodes as well, ~635 Ma Marinoan and ~580 Ma Gaskiers (Fairchild and Kennedy 2007), but the abundance of 580–710 Ma igneous activity in the region (Stern and Hedge 1985; Moussa et al. 2008) and the lack of such cobbles in the diamictite is inconsistent with deposition of the Atud diamictite during either of these younger ice ages. The Atud diamictite could be similar in age to 712 ± 1.6 Ma diamictite of the Ghubrah Formation, Oman, although the clast age populations are significantly different (Rieu et al. 2007).

Origin of pre-Neoproterozoic clasts in the diamictite and significance for diamictite formation

There is no obvious source within the Eastern Desert or NW Saudi Arabia for especially the pre-Neoproterozoic cobbles within the diamictite. Stern (2002) summarized Nd isotopic evidence that the Neoproterozoic basement of Egypt and NW Saudi Arabia is overwhelmingly a juvenile Neoproterozoic crustal addition. There are no known exposures of pre-Neoproterozoic rocks from the Eastern Desert of Egypt, Sinai, or NW Saudi Arabia. Furthermore, there are no significant exposures of ~750 Ma plutonic rocks in the immediate vicinities of the diamictite localities, although volcanic rocks of this age are increasingly being recognized in the Central Eastern Desert of Egypt (Andresen et al. 2008; Ali et al. 2008). Plutonic igneous rocks ~750 Ma are known from farther south in Sudan

and Saudi Arabia (Stern and Abdelsalam 1998; Hargrove et al. 2006a, b).

The source of at least the pre-Neoproterozoic clasts must come from outside the ophiolite-diamictite-BIF basin outlined in Fig. 1b. Dixon (1981) inferred that the 1,120–2,060 Ma cobbles within the Atud diamictite were transported from a region of pre-Neoproterozoic crust west of the Nile River, possibly by ice-rafting. This is consistent with more recent studies of Sultan et al. (1994), who reported Nd model ages of 2.85 Ga, U–Pb (zircon and sphene) and Sm–Nd whole rock crystallization ages >2.67 Ga and metamorphic ages of ~2.0 Ga for Jabal Kamil and Jabal El Asr (Fig. 1a), Western Desert of Egypt, confirming that late Archean and Paleoproterozoic crust underlies much of the region. Pre-Neoproterozoic Atud and Nuwaybah clasts could also have been derived from the SE. Stacey and Hedge (1984) reported ~1.8 Ga zircon ages for from pre-Neoproterozoic sources in the Khida terrane, Saudi Arabia. Whitehouse et al. (1998) confirmed that late Archean (2.55–2.95) crust existed in the Al-Mafid terrane of Central southern Yemen. Figure 1a shows the location of these pre-Neoproterozoic crustal tracts that could have been the source of pre-Neoproterozoic detritus for the Atud diamictite. All of these potential sites are hundreds of kilometers away from the present Atud diamictite localities.

Further insights can be obtained by comparing the age distribution of Atud diamictite ages and those of potential source regions. Figure 12 compares the distribution of pre-Neoproterozoic zircon ages for the diamictite and the pre-Neoproterozoic ages of known potential sources around the ANS from previous studies. The potential sources we consider are the Khida terrane, Yemen, and crust of the Saharan Metacraton (Abdelsalam et al. 2002) as represented by exposures west of the Nile in Egypt and at the Egypt–Sudan border at Wadi Halfa. The lack of ~2.5 Ga ages in the Khida terrane makes this an unlikely source, and the relatively subordinate abundance of ~2.0 Ga ages in Yemen makes this relatively unattractive as the source of the diamictite. The similar abundance of ~2.0 and ~ 2.5Ga ages in those parts of the Saharan Metacraton flanking the Eastern Desert is quite consistent with the distribution of ages seen in the diamictite. Further support for this potential source comes from the observation that a minor proportion of ~1.2 Ga ages are also recognized for basement of the Saharan Metacraton.

We conclude that the evidence is most consistent with an interpretation whereby the diamictite clasts were eroded from the Saharan Metacraton during a major episode of erosion and transported eastwards or northeastwards into an oceanic basin, where they were deposited. We have no direct evidence that erosional agent was glacial or that the diamictite was transport eastwards by glaciers and/or icebergs, but cannot imagine any other mechanism that is capable of eroding and transporting such large blocks of diverse lithologies such great distances. There is also a possibility that the diamictite is some kind of an impact breccia, but there is limited evidence for this interpretation. The microconglomerate clasts could be explained by such a mechanism, but we saw no evidence for shocked quartz or other evidence expected from an impact. The intensely altered nature of these rocks does not favor preservation of such features. We conclude from the above considerations that the Atud diamictite manifests the activity of Neoproterozoic glacial in the Arabian–Nubian Shield.

Conclusions

The following conclusions result from our study:

1. Units formerly referred to as Atud Conglomerate or Atud Formation in Egypt are better described as Atud Diamictite.
2. Diamictite is demonstrated for the first time from near Nuwaybah in NW Arabia. Diamictites at Wadi Kareim and Wadi Mobarak in the Eastern Desert of Egypt and in NW Saudi Arabia are correlative.
3. Atud diamictite was deposited in an oceanic basin of indeterminate size, as demonstrated by regional association with ophiolite and BIF in the Central Eastern Desert of Egypt.
4. The diamictite was deposited not long after ~750 Ma.
5. The source of clasts within the diamictite is not known but transport over several hundreds of kilometers is required. Transporting such large and lithologically diverse clasts over such large distances may have occurred by icebergs and glaciers, or formation as an impact breccia, but we prefer the suggestion that the Atud and Nuwaybah diamictite bodies are glacial deposits in the Arabian–Nubian Shield.
6. Deformation has obscured primary depositional structures, striations, and faceting so a clear glacial origin is not demonstrated. Nevertheless combined conclusions 4 and 5 strongly suggest deposition broadly Sturtian (~740–660 Ma) glacial episode in the Arabian–Nubian Shield.
7. Further studies of especially the large body of Atud/Nuwaybah diamictite near Jabal Atud are needed, as are efforts to find other outcrops in Saudi Arabia. Regional variations in the thickness of the diamictite will help constrain the direction of its source.

Acknowledgments This paper is part of the first author's Ph.D. research at the University of Texas at Dallas and was funded by NSF grant EAR- 0509486. We thank the Nuclear Materials Authority of Egypt (NMA) and the Saudi Geological Survey (SGS) for support in

the field. Special thanks go to Dr. Hani Shalaby, Dr. Hossam Khamis, Mr. Fayek Kattan, and Mr. Saad El Garney for their help during field work in Egypt and Saudi Arabia. We appreciate the assistance of Dr. Joe Wooden, Dr. Frank Mazdab and Dr. W. R. Griffin during analytical work at the SUMAC facility. Also much appreciation goes to Dr. U. S. Hargrove III for helpful advice and discussions during zircon separations. We also thank referees Dr. Nicole Dobrzinski and Dr. James Etienne and editor Prof. Wolf-Christian Dullo for insightful comments and criticisms that improved this manuscript. This is UTD Geosciences contribution number 1124.

References

Abdel Naby H, Frisch W, Hegner E (2002) Origin of Wadi Haimur–Abu Swayel gneiss belt, south Eastern Desert, Egypt: petrological and geochronological constraints. Precambrian Res 113: 307–332. doi:10.1016/S0301-9268(01)00214-5

Abdelsalam MG, Liégeois JP, Stern RJ (2002) The Saharan metacraton. J Afr Earth Sci 34:119–136. doi:10.1016/S0899-5362(02)00013-1

Abu El Ela FF (1990) Do the Atud conglomerates belong to the island arc metasediments? Bull Fac Sci Assiut Univ 19(1-F):123–155

Agar RA, Stacey JS, Whitehouse MJ (1992) Evolution of the southern Afif terrane—a geochronologic study. Saudi Arabian Deputy Ministry for mineral resource open file report DGMR-OF-10-15: 41

Akaad MK, Abu El Ela AM (1996) Geological and petrochemistry of the Muweilih submarine metabasalts, Qift–Quseir region, Eastern Desert, Egypt. Egypt J Geol 40:321–349

Akaad MK, Noweir AM (1964) A new occurrence of the Atud formation at Wadi El-Muweilih, Eastern Desert of Egypt. Bull Sci Tech Assiut Univ 7:31–48

Akaad MK, Noweir AM (1969) Lithostratigraphy of Hammamat-Um Seleimat district, Eastern Desert, Egypt. Nature 223:284–285. doi:10.1038/223284a0

Akaad MK, Noweir AM, Abu El Ela AM (1995) The volcano-sedimentary association and ophiolites of Wadi Mubarak, Eastern Desert, Egypt. Proc Int Conf Geol Surv Egypt Spec Publ 69:231–248

Akaad MK, Noweir AM, Abu El Ela AM, El-Bahariya GA (1996) The Muweilih conglomerate; Qift-Quseir road region, and the problem of the Atud formation. Presented at Proceedings of the Geological Survey Egypt, pp 23–45

Ali KA, Stern RJ, Manton WI, Kimura J-I, Khamees HA (2008) Geochemistry, Nd isotopes and U–Pb SHRIMP dating of Neoproterozoic volcanic rocks from the Central Eastern Desert of Egypt: new insights into the ~750 Ma crust-forming event. Precambrian Res (in review)

Allen PA, Leather J (2006) Post-Marinoan marine siliciclastic sedimentation: the Masirah bay formation, Neoproterozoic Huqf supergroup of Oman. Precambrian Res 144:167–198. doi:10.1016/j.precamres.2005.10.006

Allen PA, Leather J, Brasier MD (2004) The Neoproterozoic Fiq glaciation and its aftermath, Huqf supergroup of Oman. Basin Res 16:507–534. doi:10.1111/j.1365-2117.2004.00249.x

Andresen A, Abu El-Rus MA, Myhre PI, Boghdady GY, Corfu F (2008) U–Pb TIMS age constraints on the evolution of the Neoproterozoic Meatiq Gneiss dome, Eastern Desert, Egypt. Int J Earth Sci (in press)

Azer M, Stern RJ (2007) Neoproterozoic serpentinites in the Eastern Desert, Egypt: fragments of fore-arc mantle. Geology 115:457–472. doi:10.1086/518052

Boulton GS (1978) Boulder shapes and grain size distributions of debris as indicators of transport paths through a glacier and till genesis. Sedimentlogy 25:773–799. doi:10.1111/j.1365-3091.1978.tb00329.x

Bowring SA, Grotzinger JP, Condon DJ, Ramezani J, Newall M, Allen PA (2007) Geochronologic constraints on the chronostratigraphic framework of the Neoproterozoic Huqf supergroup, Sultanate of Oman. Am J Sci 307:1097–1145. doi:10.2475/10.2007.01

Corfu F, Hanchar JM, Hoskin PW, Kinny P (2003) Atlas of zircon textures. Rev Mineral Geochem 53:469–500. doi:10.2113/0530469

Davies FB (1985) Geological map of the Al Wajh Quadrangle, Sheet 26B, Kingdom of Saudi Arabia, Ministry of petroleum and mineral resources, Kingdom of Saudi Arabia

Dixon TH (1979) The evolution of continental crust in the late Precambrian Egyptian Shield. (Ph.D. thesis): University of California, San Diego, p 231

Dixon TH (1981) Age and chemical characteristics of some Pre-Pan-African rocks in the Egyptian Shield. Precambrian Res 14:119–133. doi:10.1016/0301-9268(81)90017-6

El-Essawy MA (1964) Geology of the area east of Gabal Atud, Eastern Desert, Egypt. [M.Sc. thesis]: Assiut University, Assiut, p 235

Eyles N, Januszcak N (2004) 'Zipper-rift': a tectonic model for Neoproterozoic glaciations during the breakup of Rodinia after 750 Ma. Earth Sci Rev 65:1–73

Fairchild IJ, Kennedy MJ (2007) Neoproterozoic glaciation in the earth system. J Geol Soc London 64:895–921

Flint RF, Sanders JE, Rodgers J (1960) Diamictite, a substitute term symmictite. Geol Soc Am Bull 71:1809–1810

Goldring DC (1990) Banded iron formation of Wadi Sawawin district, Kingdom of Saudi Arabia. Tran Instn Min Metall (Sect B: Appl Earth Sci) 99: B1–B14

Hambrey MJ, Glasser NF (2002) Development of landform and sediment assemblages at maritime high-Arctic glaciers. In: Hewitt K (ed) Landscapes of transition. Kluwer, Dordrecht, pp 11–42

Hargrove USI, Stern RJ, Griffin WR, Johnson PR, Abdelsalam MG (2006a) From island arc to craton: timescales of crustal formation along the Neoproterozoic Bi'r Umq suture zone, Kingdom of Saudi Arabia. Saudi Geological Survey Technical Report SGS-TR-2006-6: 69

Hargrove US, Stern RJ, Kimura JI, Manton WI, Johnson PR (2006b) How juvenile is the Arabian–Nubian Shield? Evidence from Nd isotopes and pre-Neoproterozoic inherited zircon in the Bi'r Umq suture zone, Saudi Arabia. Earth Planet Sci Lett 252:308–326

Hoffman PF (2007) Comment on "Snowball Earth on trial". EOS 88(9):110

Jacobs J, Thomas RJ (2004) Himalayan-type indenter-escape tectonics model for the southern part of the late Neoproterozoic-early Paleozoic east African–Antarctic Orogen. Geology 32:721–724

Kennedy A, Johnson PR, Kattan FH (2004) SHRIMP geochronology in the northern Arabian Shield. Part I: Data acquisition. Saudi Geological Survey Open File Report, SGS-OF–2004-11

Kennedy A, Johnson PR, Kattan FH (2005) SHRIMP geochronology in the northern Arabian Shield. Part II: Data acquisition 2004. Saudi Geological Survey Open File Report, SGS-OF-2005-10

Kennedy A, Johnson PR, Kattan FH (2007) SHRIMP geochronology in the northern Arabian Shield: Part III Data Acquisition 2006. Saudi Geological Survey, Jeddah (in press)

Kröner A, Sassi FP (1996) Evolution of the northern Somali basement: new constraints from zircon ages. J Afr Earth Sci 22:1–15

Kröner A, Todt W, Hussein IM, Mansour M, Rashwan AA (1992) Dating of late Proterozoic ophiolites in Egypt and the Sudan using the single zircon evaporation technique. Precambrian Res 59:15–32

Le Guerroué E, Allen PA, Cozzi A (2005) Two distinct glacial successions in the Neoproterozoic of Oman. GeoArabia 10: 17–34

Leather J (2001) Sedimentlogy, chemostratigraphy and geochronology of the lower Huqf Supergroup, Oman (Ph.D. thesis): Trinity College, Dublin, p 227

Ludwig KR (2000) Isoplot/Ex 3.0: a geological toolkit for Microsoft EXCEL. Berkeley Geochronology Center Special Publication, 1a: 1–54

Moghazi AM (2003) Geochemistry and petrogenesis of a high-K calc-alkaline Dokhan volcanic suite, South Safaga area, Egypt: the role of late Neoproterozoic crustal extension. Precambrian Res 125:161–178

Moussa EM, Stern RJ, Manton WI, Ali KA (2008) SHRIMP zircon dating and Sm/Nd isotopic investigations of Neoproterozoic granitoids, Eastern Desert, Egypt. Precambrian Res 160:341–356

Mukherjee SK, Stern RJ, Ali KA, Miller NR, Johnson PR, Whitehouse MJ (2009) Petrology, age (U–Pb zircon) and geochemistry of Sawawin banded iron formation, NW Arabia-implications for the Neoproterozoic climate change controversy. Precambrian Res (submitted)

Ovenshine AT (1970) Observations of iceberg rafting in Glacier bay, Alaska, and the identification of ancient ice-rafted deposits. Geol Soc Am Bull 81:891–894

Ries AC, Shackelton RM, Graham RH, Fitches WR (1983) Pan African structures, ophiolites and melange in the Eastern Desert of Egypt: a traverse at 26 N. J Geol Soc London 140:75–95

Rieu R, Allen PA, Cozzi A, Kosler J, Bussy F (2007) A composite stratigraphy for the Neoproterozoic Huqf supergroup of Oman: integrating new litho-, chemo- and chronostratigraphic data of the Mirbat area, southern Oman. J Geol Soc London 164:997–1009

Shalaby A, Stuwe K, Makroum F, Fritz H, Kebede T, Klotzli U (2005) The Wadi Mubarak belt, Eastern Desert of Egypt: a Neoproterozoic conjugate shear system in the Arabian–Nubian Shield. Precambrian Res 136:27–50

Sims PK, James HL (1984) Banded iron-formations of late Proterozoic age in the Central Eastern Desert, Egypt: geology and tectonic setting. Econ Geol 79:1777–1784

Stacey JS, Agar RA (1985) U–Pb isotopic evidence for the accretion of a continental microplate in the Zalm region of the Saudi Arabian Shield. J Geol Soc London 142:1189–1203

Stacey JS, Hedge CE (1984) Geochronologic and isotopic evidence for early Proterozoic crust in the Eastern Arabian Shield. Geology 12:310–313

Stern RJ (1979) Late Precambrian ensimatic volcanism in the Central Eastern Desert of Egypt. Ph.D. thesis. University of California, San Diego, CA, p 210

Stern RJ (1981) Petrogenesis and tectonic setting of late Precambrian ensimatic volcanic rocks, Central Eastern Desert of Egypt. Precambrian Res 16:197–232

Stern RJ (1994) Arc assembly and continental collision in the Neoproterozoic east African Orogen: implications for the consolidation of Gondwanaland. Annu Rev Earth Planet Sci 22:319–351

Stern RJ (2002) Crustal evolution in the east African Orogen: a Neodymium isotopic perspective. J Afr Earth Sci 34:109–117

Stern RJ, Abdelsalam MG (1998) Formation of juvenile continental crust in the Arabian–Nubian Shield: evidence from granitic rocks of the Nakasib suture, NE Sudan. Geol Rundsch 87:150–160

Stern RJ, Hedge CE (1985) Geochronologic and isotopic constraints on late Precambrian crustal evolution in the Eastern Desert of Egypt. Am J Sci 285:97–127

Stern RJ, Kröner A, Bender R, Reischmann T, Dawoud AS (1994) Precambrian basement around Wadi Halfa, Sudan: a new perspective on the evolution of the east Saharan craton. Geol Rundsch 83:564–577

Stern RJ, Avigad D, Miller NR, Beyth M (2006) Evidence for the Snowball Earth hypothesis in the Arabian–Nubian Shield and the east African Orogen. J Afr Earth Sci 44:1–20

Sultan M, Becker R, Arvidson RE, Shore P, Stern RJ, El Alfy Z, Attia R (1993) New constraints on Red Sea rifting from correlations of the Arabian and Nubian Neoproterozoic outcrops. Tectonics 12:1303–1319

Sultan M, Tucker RD, El Alfy Z, Attia R, Ragab AG (1994) U–Pb (zircon) ages for the gneissic terrane west of the Nile, southern Egypt. Geol Rundsch 83:514–522

Tera F, Wasserburg GJ (1972) U–Th–Pb systematics in three Apollo 14 basalts and the problem of initial Pb in lunar rocks. Earth Planet Sci Lett 14:281–304

Walraven F, Rumvegeri BT (1993) Implications of whole-rock Pb–Pb and zircon evaporation dates for the early metamorphic history of the Kasai craton, southern Zaire. J Afr Earth Sci 16:395–404

Wetherill GW (1956) Discordant uranium–lead ages I. Trans Am Geophys Union 37:320–326

Whitehouse MJ, Windley BF, Ba-Bttat MA, Fanning CM, Rex DC (1998) Crustal evolution and terrane correlation in the Eastern Arabian Shield, Yemen: geochronological constraints. J Geol Soc London 155:281–295

Whitehouse MJ, Stoeser DB, Stacey JS (2001a) The Khida terrane—geochronological and isotopic evidence for Paleoproterozoic and Archean crust in the Eastern Arabian Shield of Saudi Arabia (extended abstract). Gondwana Res 4(2):200–202

Whitehouse MJ, Windley BF, Stoeser DB, Al-Khirbash S, Ba-Bttat MA, Haider A (2001b) Precambrian basement character of Yemen and correlations with Saudi Arabia and Somalia. Precambrian Res 105:357–369

Wilde SA, Youssef K (2000) Significance of shrimp U–Pb dating of imperial porphyry and associated Dokhan volcanics, Gebel Dokhan, north Eastern desert, Egypt. J Afr Earth Sci 31:403–413